LOCOMOTION CHARACTERIZATION OF DCC AND NCK2 MUTANT MICE

by

Qingyu Li

Submitted in partial fulfillment of the requirement

for the degree of Master of Science

at

Dalhousie University

Halifax, Nova Scotia

September 2016

TABLE OF CONTENTS

LIST OF FIGURES

LIST OF TABLES

LIST OF ABBREVIATIONS USED

BF	Bicep Femoris
BMP	Bone Morphogenic Proteins
BrdU	Bromodeoxyuridine
C#	Cervical Segment
C57BL6	C57 Black6 Mouse Strain
CBLN4	Cerebellin 4
CDC42	Cell Division Control Protein 42 Homolog
$cDCC^{f/-}$	$Hoxb8::cre^{+/-};DCC^{f/-}$
$cDCC^{f/+}$	$Hoxb8::cre^{+/-};DCC^{f/+}$
$cDCC^{f/f}$	$Hoxb8::cre^{-/-};DCC^{f/f};TdTomato^{+/-}$
cDNA	Complementary DNA
CNS	Central Nervous System
CPG	Central Pattern Generator
CST	Corticospinal Tract
Dab1	Disabled-1
Dbx1	Developing Brain Homeobox 1
DCC	Deleted in Colorectal Cancer
DF	Dorsal Faniculus
dI	Dorsal Born Interneuron
Draxin	Dorsal Repulsive Axon Guidance Protein
DV	Dorsoventral
E#	Embryonic Day
E1	Ankle Extensor Phase I
E2	Ankle Extensor Phase II
E3	Ankle Extensor Phase III

EGF	Epidermal Growth Factor
En1	Engrailed-1
Evx	Even-Skipped Homeobox
F	Ankle Flexor Phase
FN1-6	Fibronectin Type III Domains
FYN	FYN Oncogene Related to SRC, FGR, YES
GABA	Gamma-Aminobutyric Acid
GEF	Guanine Nucleotide Exchange Factor
GS	Gastrocuemius-soleus
Hip E	Hip Extensor Phase
Hip F	Hip Flexor Phase
Hoxb8	Homeobox B8
Ig	Immunoglobulin
IgSF	Immunoglobulin Super Family
IN	Interneurons
IP	Iliopsoas
KO	Knockout
L#	Lumbar Segment
Lbx1	Ladybird Homeobox 1
Lhx	LIM Homeobox
LN	Liminin-like Domain
LTP	Long Term Potentiation
$mDCC^{f/-}$	$Hoxb8::cre^{+/-};DCC^{f/-}$
$mDCC^{f/f}$	$Hoxb8::cre^{+/-};DCC^{f/f};TdTomato^{+/-}$
MM	Congenital Mirror Movement Disorder
NA	Nipecotic Acid
NCK	Non-Catalytic Region of Tyrosine Kinase Adaptor Protein

PAK	P21 Activated Kinase
Pax2	Paired Box 2
pY	Phosphorylated Tyrosine
RA	Retinoic Acid
RabGDI	Rab Guanine Nucleotide Dissociation Inhibitor1
RAC1	Ras-related C3 Botulinum Toxin Substrate
Robo	Roundabout Receptor
SH2	Src-homology 2
SH3	Src-homology 3
Shh	Sonic Hedgehog
Sim1	Single-minded Homolog 1
TA	Tibialis Anterior
TF	Transcription Factor
TRIO	Triple Functional Domain Protein
V#	Ventral Spinal Interneuron Population
WASP	Wiskott–Aldrich Syndrome Protein

ABSTRACT

Transmembrane receptor protein DCC (deleted in colorectal cancer) and its intracellular binding partner Nck (non-catalytic tyrosine kinase adaptor protein) are both important in spinal locomotor network formation. Depletion of DCC or both Nck proteins cause altered left-right coordination. The distinct function of Nck1 and Nck2 and their relation to DCC in locomotion is unclear. A novel genetic mutation method enabled us to study the locomotion in adult DCC deficient and Nck2 knockout mice. DCC deficiency in the spinal cord causes hindlimb synchronization, and a decrease in locomotion speed caused by decreased stride length, which is partially compensated by increased stride frequency. Nck2 depletion causes elongated swing duration and increased ankle flexor and extensor 1 phase, accompanied by in phase elongation of flexor muscle activation and more abrupt extensor muscle activation. The distinct phenotypes of the mutant animals indicate Nck2's distinct role in locomotion through partially DCC-independent pathway.

CHAPTER 1 INTRODUCTION

Locomotion in animals involves neuronal control at different levels of the nervous system. During rhythmic and coordinated activities like walking, local neuronal networks in the spinal cord are responsible for the generation of correct limb or body movement. Such neuronal network that is in charge of rhythm generation, inter- and intra-limb coordination is referred to as central pattern generators (CPGs). A functional CPG consists of many different types of interneurons. The proper formation of CPG requires all these interneuron populations not only to exist in proper numbers and possess certain intrinsic properties, but also to form correct connection to each other to establish the functional network.

One of the important processes required for the proper connection between different interneuron populations is axon guidance. Axon guidance is a complicated process which involves not only the release of different attractive and repellent signals in the spinal cord, but also the differential expression of appropriate receptors on the surface of the targeted cells, which would trigger proper downstream signaling pathways. The collective acts of these molecular interactions result in the correct pathfinding of the axons and therefore a functional CPG network.

Both DCC (deleted in colorectal cancer) and NCK (non-catalytic region of tyrosine kinase adaptor) have been indicated that they play important roles in the development of locomotor circuits in the spinal cord. Deletion of DCC or both NCK1 and 2 in the nervous system disrupts the left-right coordination in the animals (Fawcett et al., 2007;

Bernhardt et al., 2012). It was suggested that DCC signaling might function through NCK1 and NCK2 (Lane, Qi and Fawcett, 2015). However, the precise function of these molecules in locomotion, especially in adult animals, have yet been well understood.

In this study, we have employed a new genetic strategy to specifically modify the expression of DCC in the caudal region of the body, which allows us to separate DCC's function in local spinal cord and higher levels of the nervous system and study its function of locomotor activity in adult animals. It also provides an opportunity to look at the influence of dosage effect at these levels by comparing the different heterozygous strains. Furthermore, we analyzed locomotion behavior of NCK2 single knockout adult animals on treadmills. This is the first time that the locomotion of Nck2 single knockout has been described in detail. Our results showed that DCC deficiency and Nck2 depletion generated completely different gate deficits, which indicates that they might play different roles in the formation of locomotion circuits.

1.1 Overview of CPG and Control of Limbed Locomotion

1.1.1 The Development of Spinal Interneurons in Locomotor CPGs

During early development of the spinal cord, the graded activity of several signaling molecules including sonic hedgehog (Shh), bone morphogenic proteins (BMPs), retinoic acid (RA) and Wnts and the consequential expression of patterning factors determined the boundary of different progenitor domains along the dorsoventral (DV) axis (Chiang et al., 1996; Liem et al., 1997; Timmer et al., 2002 and reviewed in Jessell, 2000). The combination of the patterning factors give rise to progenitor domains of MNs and eleven subpopulations of spinal interneurons (INs, Goulding, 2009 Figure 1A).

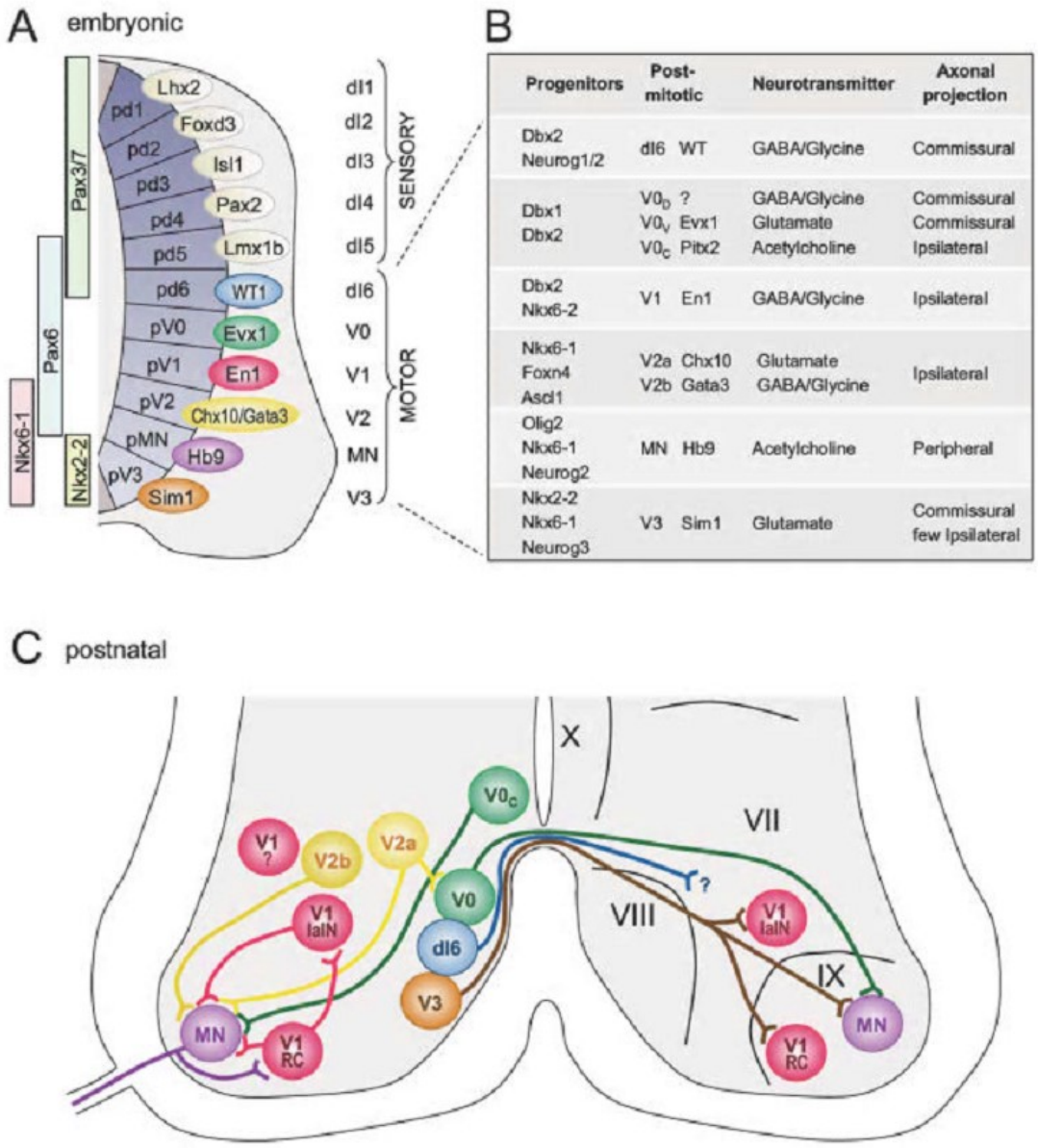

Figure 1. Spinal Interneuron Population and Development

Early development schematic of eleven progenitor domains (pd1-pV3) along the dorsoventral axis of the mouse spinal cord (A). Eleven postmitotic neuronal populations arise from the domains. Physiological properties and transcription factor expression pattern in these populations are outlined in (B). Schemetic spinal motor circuitry shows the location of interneuron population and their subsets and connections according to the current understanding. p, progenitor domain. Adapted from Grossmann et al., 2010.

The locomotor CPGs are located in the ventral spinal cord (Goulding, 2009), including motor neurons and interneurons mainly derived from ventral progenitors, pV0-pV3. These progenitor cells later develop into five post-mitotic subpopulations, denoted as V0, V1, V2a, V2b, and V3 interneurons (INs, Figure 1B,C, Jessell, 2000; Goulding, 2009). These subpopulations are identified by the expression of unique transcription factors (TFs), for examples, Evx1/2 in V0 INs, En1 in V1, Chx10 in V2a, Gata2/3 in V2b and Sim1 in V3 (Saueressig et al., 1999; Moran-Rivard et al., 2001; Karunaratne et al., 2002; Kimura et al.,2006; Al-Mosawie et al., 2007; Lundfald et al., 2007; Peng et al., 2007; Crone et al., 2008; Zhang et al., 2008; reviewed in Jessell, 2000; Goulding, 2009 and Figure 1B). Recently, it has been shown that dorsally derived INs can also be involved in the CPG networks, such as dI6 neurons marked by Dmrt 3 and/or wt1 , are also believed to contribute to CPG network (Gross et al., 2002; Muller et al., 2002; Vallstedt A, Kullander K, 2013).

The above major classes of ventral spinal interneurons can be further divided into subtypes. Two subtypes of V0 interneurons exist. The Evx1/2^{-} dorsal subtype, or $V0_D$, which makes up 70% of the V0 population, are inhibitory interneurons that project onto contralateral motor neurons. The Evx1/2^{+} ventral subtype, or $V0_V$, which makes up the rest 30% of the V0 population, are excitatory interneurons that give excitatory input into contralateral motor neuons (Jessell, 2000; Moran-Rivard et al., 2001; Pierani et al., 2001; Lanuza et al., 2004; Goulding, 2009). The V1 population is made up all inhibitory neurons, but can be further divided into 10% of Renshaw cells (RCs), characteristic of their expression of Nicotinic cholinergic receptor alpha 2 (Chma2), 20% of rIa-INs, and another 70% of neurons that are functionally unclear (Alvarez et al., 2005; Goulding,

2009). The Ipsilateral projecting V2 population can be divided into $Chx10^+$ V2a-INs, an excitatory subtype that project onto V0v-INs, MNs and V2a-INs themselves, as well as $Gata2/3^+$ V2b-INs, an inhibitory subtype that includes some rIa-INs (Al-Mosawie et al., 2007; Lundfald et al., 2007; Crone et al., 2008; Goulding, 2009; Crone et al., 2009; Dougherty and Kiehn, 2010; Zhong et al., 2010; Siembab et al., 2010). The excitatory V3 population can also be divided into two subtypes, with the majority subtype (85%) projecting to controlateral MNs, RCs and rIa-INs and the minority (15%) projecting to Ipsilateral V2-INs (Zhang et al., 2008; Kiehn et al., 2010).

The knowledge of the TF profiles in different spinal neurons has enabled us to genetically track and manipulate specific subpopulations of INs to reveal their functions in locomotor activities. Such studies have shown that each of these ventrally-located interneuron subpopulations in the spinal cord plays unique roles in locomotor circuits. For example, commissure V0-INs are believed to control the left-right alternation during locomotion. More specifically, $V0_D$-INs are responsible for the left-right alternation under lower frequency, while $V0_V$-INs are important at higher speed (Pierani et al., 2001; Lanuza et al., 2004; Talpalar et al., 2013). The ipsilaterally projecting excitatory V2a-INs are also in control of left-right coordination by providing rhythmic excitatory input to V0-INs (Crone et al., 2008). Ipsilaterally projecting inhibitory V1-INs, on the other hand, are believed to affect the speed of locomotion by regulating burst initiation and termination in each step cycle (Gosgnach et al., 2006; Betley et al., 2009, Sapir et al., 2004 and Saueressig et al., 1999). Recent studies also suggest that V1-INs regulate the flexor-extensor coordination together with inhibitory V2b-INs (Zhang et al. 2014).

Furthermore, the contralaterally projecting excitatory V3-INs are related to the robustness and balance of the locomotor outputs (Zhang et al., 2008).

1.1.2 The Function of CPG in Control of Coordination During Locomotion

In limbed locomotion, CPG is in charge of two types of coordination: left-right coordination and flexor-extensor coordination. Both types of coordination have been studied intensively, and neuronal network models have been proposed (Figure 2).

Left-right coordination necessarily involves commissural interneurons that project to the contralateral side. Under different locomotion speed, both left-right alternating and left-right synchronized movement appear in wildtype rodent, suggesting networks controlling both modes exist. It has been widely accepted that the left-right alternating movement is the result of a dual inhibitory pathway in the spinal cord, which consists of inhibitory commissural interneurons (CINi) projecting directly to contralateral motor neurons (MNs), or direct pathway, and excitatory commissural interneuorns (CINei) inhibiting contralateral MNs indirectly via other inhibitory interneurons, or indirect pathway. The dual inhibitory pathway is active at lower speeds, resulting in alternating movement such as walking. Loss of function studies suggest that V0 an V2a INs are essential for left-right alternation. V0 subpobulations V0V act via indirect pathway (Figure 2A), and V0D via direct pathway (Figure 2A, Kiehn et al., 2010). V2a-INs project to the indirect pathway while rhythm-generating neurons drive the direct pathway (Dougherty & Kiehn, 2010 Figure 2A). Anatomical evidences also suggest that a subpopulation of V3 INs may also play roles in left-right alternation via indirect pathway due to their projection to inhibitory neurons (Figure 2A, Kiehn et al., 2010).

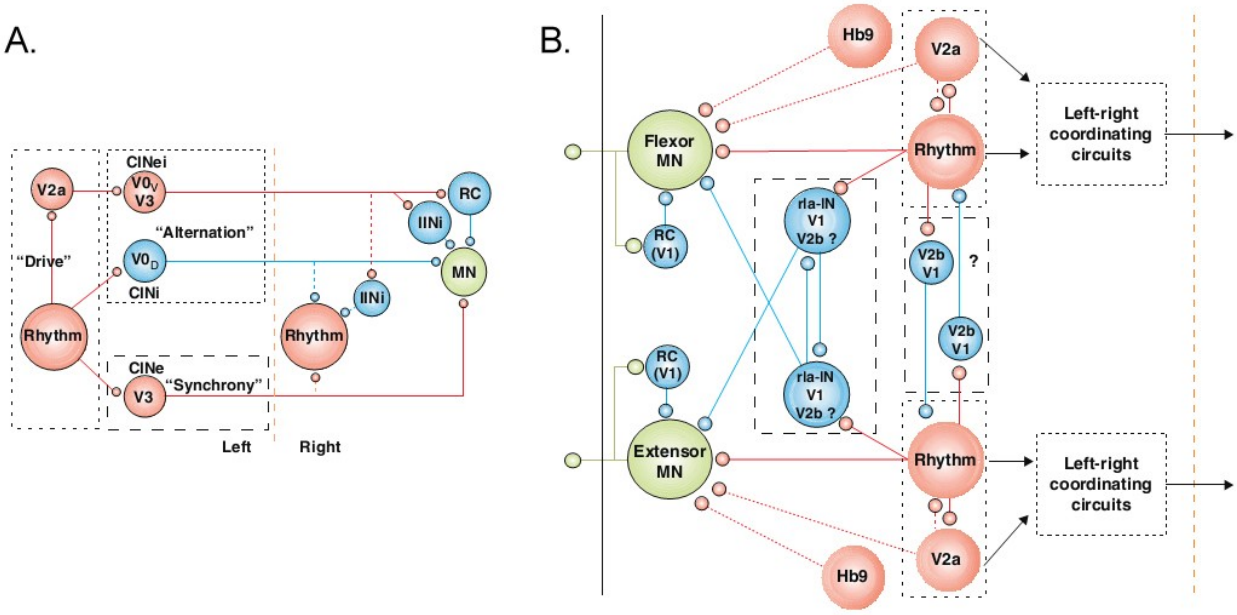

Figure 2. CPG Model of Left-Right and Flexor-Extensor Coordination in Limbed Locomotion

(A) Proposed model of secmental rodent CPG for control of left-right coordination. Left-right alternation is achieved by the activation of the direct pathway, involving the direct inhibition of contralateral MNs by inhibitory CINs, and the indirect pathway, involving the inhibition of contralateral MNs by excitatory CINs via inhibitory INs. Left–right synchrony is achieved by activation of excitatory CINs that project to contralateral MNs. The crossed connections are also connected to contralateral rhythm-generating center and/or corresponding CINs to achieve left-right coordination. Multiple ipsilateral excitatory neurons including V2a INs mediates the drive of left-right coordination pathways. (B) Proposed model of the segmental rodent CPG for control of flexor-extensor coordination. Alternating excitation and inhibition drive flexor and extensor MNs to rhythmic firing. Excitatory rhythm-generating neurons drive inhibitory premotor neurons. Ia INs, reciprocally connected inhibitory premotor neurons originating from V1 and possibly V2b INs, are indicated as candidate responsible inhibitory neurons by electrophysiological and genetic studies (box: rIa-IN, V1 and V2b?). Non-reciprocal group I INs are also involved (not shown). Some rhythmic premotor inhibition is mediated via V1 related RCs activity and crossed connections (shown in (A)). V2a-INs

connect to MNs and, although dispensable for rhythm-generation, may also have connecting to the ipsilateral rhythm-generating core. Other excitatory ipsilateral neurons including Hb9 and ipsilateral V3 and unidentified INs are responsible for rhythm generation (not shown). Between flexor and extensor rhythm-generating centers, inhibitory reciprocal connections are proposed hypothetically (box: V1, V2b?) to strengthen flexor–extensor alternation. Candidate responsible neurons are V1 and V2b originated INs apart from reciprocal Ia INs or RCs. IN = interneurons; CINe = excitatory commissure interneurons; CINi = inhibitory commissure interneurons; IINi = ipsilaterally projecting inhibitory interneuron. RC=Renshaw Cell. MN=motor neuron. Inhibitory neurons are blue. Excitatory neurons are red. MNs are green. Red dotted lines are the midline. Adapted from Kiehn, 2011.

The left-right synchronized movement is believed to be the result of CINs (CINe) projecting directly to contralateral MNs, which is active at higher speeds, causing the animal to hop. V3-CINs are believed to be largely responsible for the left-right synchronization, since the majority of them give direct excitatory input to contralateral MNs (Keihn, 2011).

The flexor-extensor alternation is essential in limbed locomotion since it ensures the coordination of joints. Flexor and extensor MNs both receive alternating excitatory and inhibitory drive during locomotion. Therefore, inhibitory neurons with monosynaptic connections to MNs are the central element that secures the reciprocal connection between flexor and extensor modules (Endo and Kiehn, 2008; Nishimaru and Kakizaki, 2009). The identity of these inhibitory neurons projecting monosynaptically to ipsilateral MNs have been indicated as RCs, rIa-INs, and non-reciprocal group I INs (Nishimaru and Kakizaki, 2009; Wang et al., 2008; Wilson, Blagovechtchenski and Brownstone, 2010). RCs receive excitatory input from MNs and inhibit the same MNs that activate them (Nishimaru and Kakizaki, 2009). rIa-INs are a group of neurons inhibiting the antagonist MNs, so named because they are activated by group Ia afferents from the corresponding muscle spindles. Flexor and extensor related rIa-INs also inhibit each other reciprocally (Wang et al., 2008). However, eliminating V1 INs, 30% of which are RCs and rIa-INs (Goulding, 2009), did not manage to eliminate the rhythmic inhibition in MNs (Velasquez et al., 2006), indicating the heterogeneity of rIa-INs (Siembab et al., 2010). It has been suggested that part of the rIa-IN population is generated from V2b-INs (Goulding, 2009; Lundfald et al., 2007). In addition, another inhibitory IN population in the dorsal cord as

well as some CINs are also indicated to be involved in the rhythmic inhibition of MNs (Figure 2B, Grillner, 2003; Wilson, Blagovechtchenski and Brownstone, 2010).

1.1.3 Sensory Feedback in the Spinal Cord During Locomotion

Sensory feedback plays an important role in adjusting locomotion although CPG can operate without it (Pearson, 2004; reviewed by Grillner, 1981; Rossignol, 1996; Orlovsky et al. 1999; Rossignol et al. 2006). Sensory feedback to the spinal cord during locomotion is composed of proprioceptive and cutaneous feedback.

Part of the proprioceptive feedback comes from group I afferents, which consists of Ia muscle spindle afferents and Ib golgi tendon organ afferents, the function of which is better understood. Group I afferents activation leads to strong excitation of the antagonist MNs (Conway et al. 1987; Pearson & Collins, 1993; Guertin et al. 1995; Perreault et al. 1995; Stecina et al. 2005). Activities of group I afferents are important in regulating stance duration and controlling the stance to swing transition (Duysens & Pearson, 1980; Pearson, 2004; Rossignol et al. 2006). Another part of the proprioceptive feedback comes from group II afferents, which is less understood. Group II afferents activation in the extensor nerves has minimal effect on locomotion (Conway et al. 1987; Guertin et al. 1995; Donelan & Pearson, 2004). In contrast, activation of the flexor group II afferents has strong effect on MN activity, and can either prolong or terminate flexion in fictive locomotion (Perreault et al. 1995; Stecina et al. 2005), and usually enhances flexor activity during treadmill locomotion (Hiebert et al. 1996). Apart from proprioceptive feedback, cutaneous feedback is also important in the control of locomotion(Zehr & Duysens, 2004; Rossignol et al. 2006). Stimulation of tibial cutaneous afferents during

extension increases extensor MNs activity and prolongs extension, while same stimulation during flexion initiates extension prematurely during fictive locomotion (Conway et al. 1994; Guertin et al. 1995).

It is important to notice that both proprioceptive and cutaneous feedback afferents regulate locomotion by projecting both directly to MNs and through CPG to antagonist MNs(Conway et al. 1987; Gossard et al. 1994; McCrea, 2001; Pearson, 2004; Rossignol et al., 2006; Quevedo et al. 2005a; Quevedo et al. 2005b). The circuits of spinal CPG and reflex are integrated, enabling mutual influence and modification (Jankowska et al. 1967; McCrea, 2001; Angel et al. 2005). In principle, sensory feedback during locomotion helps the animal to adjust to their physical environment with minimal interruption of rhythmic locomotion itself.

1.1.4 Descending Signals in Locomotion

In additional to sensory feedback, another factor worth noticing in locomotion is the function of descending input. The supraspinal signals is critical to adapt the basic locomotion pattern to the terrain as well as to the initiation and control of locomotion (Drew et al., 2004). The major sources of supraspinal signals are divided into two systems (Lawrence and Kuypers, 1968a,b). The lateral system consists of corticospinal tract (CST) and rubrospinal tract, and is important in adjusting the fine movement in locomotion to the physical environment. CST conveys signals from the motor cortex to CPG in the spinal cord, and is important in voluntary adjust of locomotion pattern, such as in response to visual stimulation (reviewed by Rossignol, 1996). The medial system consists of reticulospinal tract and vestibulospinal tract. The reticulospinal neurons receive signals

from mesencephalic locomotor region and lateral hypothalamus and project to spinal cord CPG, and also play important roles in the initiation of locomotion (Whelan, 1996). It is important to notice that descending neurons can project either directly to MNs or indirectly via premotor or interneurons (reviewed by Drew et al., 2004). Therefore, all the supraspinal signals are integrated at the spinal level with CPG and afferent signals.

1.1.5 The Significance of Step Cycle and Joint Angle Analysis in Locomotion Studies

In the study of limbed locomotion, the analysis of step cycle and joint angle cycle have long been used to reveal problems with coordination, since changes in step cycle or joint angles are correlated and reveal changes in muscle activation.

The step cycle and joint angle cycle during the locomotion of wildtype intact mouse have been described in detail (Leblond et al., 2003). The step cycle of the intact mouse refers to the time starting from the foot contacts the ground to its next contact with the ground. A step cycle can be divided into a stance phase and a swing phase. The stance phase starts from the foot's contact with the ground and ends at the initiation of the forward movement. The swing phase starts from the beginning of the foot's forward movement and ends when it contacts the ground again. In general, the switch from stance to swing phase coincides with the moment the foot leaves the ground. However, in some cases, the paw of the mouse drags on the ground at the beginning of the swing phase. It should be noted that the duration of the drag should be included in the swing phase, since the foot is already starting to move forward as a result of flexion.

Step cycle is further divided into subdivisions according to the change of joint angles as describe by Philippson (1905). The decrease of a particular joint angle indicates the flexion of the corresponding joint, and the increase of that angle indicated joint extension. In wildtype mice, the hip joint flexion, or the hip flexor phase (Hip F), corresponds to the swing phase since the hip joint angle decreases as the foot moves forward. Consequently, the hip joint extension, or hip extensor phase (Hip E), corresponds to the stance phase since the hip joint angle increases as the foot moves backwards.

The change of the ankle joint angle can be divided into four phases. At the beginning of the swing, the ankle angle decreases as the ankle joint flexes together with the hip joint to lift the foot. The duration of this ankle joint angle decrease is referred to as the ankle flexor phase (F). The ankle flexor phase is followed by ankle extensor phase 1 (E1), when ankle angle increases as the ankle and knee joints extend while the hip joint continues the flexion, which brings the foot to the ground. When the paw contacts the ground, extensor phase 2 (E2) begins as ankle joint angle starts to decrease again while hip joint starts extension. Extensor phase 3 (E3) begins when ankle joint starts to extend and ends with its next flexion at the beginning of swing, during which the hip and knee joints also extend so the body of the mouse is propelled forward.

1.2 Overview of Axon Pathfinding in CPG Formation

In addition to the development of neuronal subpopulation identity, the formation of spinal locomotor circuits involves another crucial event: the migration of each neuronal subtype to their destined location. An essential part of migration is axon guidance.

Navigating axons has an enlarged terminal structure, the growth cone, which is composed of a central microtubule domain and a peripheral actin-rich lamellipodia and filopodia domain, allowing it to change the shape in response to extracellular cues (Bashaw and Klein, 2010; Raper and Mason, 2010; Vitriol and Zheng, 2012). Many different types of receptors exist on the growth cone surface, which can be activated by their corresponding ligands, the extracellular guidance molecules. The activation of these receptors initiate series of downstream signaling that eventually lead to the remodeling of the cytoskeleton of the growth cone, and thus the attractive or repelling effect, depending on their molecular nature (Vitriol and Zheng, 2012). Therefore, the spatial and temporal expression of different receptors on the growth cone as well as their responsiveness and downstream signaling all affect an axon's navigation in its physiological environment, thus contributing to the extreme complexity of spinal locomotor network formation.

One of the best understood models of axon guidance in spinal locomotor network formation is the spinal commissure formation. The axon guidance involved in spinal commissure formation can be roughly divided into three stages: precrossing, crossing and postcrossing (reviewed by Castellani, 2013). During the precrossing stage, axons from dorsally born populations navigate toward the ventral part of the cord under the combined influence of roof plate secreted chemorepellents and floor plate secreted chemoattractants. After the axons reach the ventral part of the spinal cord, commissure axons continue to cross the midline due to their responsiveness to floor plate chemoattractants and lack of responsiveness to the floor plate chemorepellents. After the axons cross the midline, their receptors to the chemoattractants became non responsive while receptors to chemorepellents are activated, so the commissure axons leave the midline to reach the

other side of the cord without recrossing. Axons from the ipsilateral populations however, are responsive to the floor plate secreted chemorepellents from the beginning, and therefore stay on the original side. During the postcrossing stage, the commissure axons are navigated rostrally or caudally under the effects of adhesive molecules and longitudinal chemoattractants and chemorepellents. In the following part, we will mainly focus on several ligand-receptor pairs involved in precrossing and crossing stages, including Netrin-DCC, slit-Robo and Ephrin-Eph, and discuss their function in spinal commissure and locomotor network formation (simplified illustration in Figure 3D).

Netrin 1, derived from the floor plate, is a diffusible chemoattractant for commissural neuron axons (Serafini et al., 1994). It elicits its effect by activating its major receptor DCC, which is expressed on the growth cone surface of most commissure neurons (Serafini et al., 1996; Fazeli et al., 1997). In vertebrates, Netrin 1 forms a concentration gradient along the dorsal-ventral axis of the developing spinal cord, with the highest concentration at the floor plate (Kennedy et al., 2006). Axons expressing DCC at their surface are attracted toward higher Netrin concentration. Therefore, the chemoattraction of Netrin 1 on DCC expressing axons is long distance, and plays an important role in the precrossing stage of spinal commissure formation.

The slit proteins are another family of diffusible proteins secreted from the floor plate, majorly eliciting repulsion on commissure axons expressing their receptors, Robo (Long et al., 2004). The Slit-Robo mediated repulsion plays an important role during the crossing stage of spinal commissure formation. While the Robo receptors expressed on the ipsilateral axons react to slit repulsion from the beginning, Robo receptors on

commissure neurons are initially nonresponsive to slit until they cross the midline (Saxena et al., 2012). Several theories are proposed to explain this change of responsiveness, including the proteolytic processing, ubiquitination, and Rab Guanine Nucleotide Dissociation Inhibitor1 (RabGDI) mediated vesicle fusion machinery change of Robo receptors at the midline (Yuasa-Kawada et al., 2009; Coleman et al., 2010; Philipp et al., 2012).

The Ephrin-Eph is another ligand-receptor pair that mediates spinal commissure formation, as well as the midline crossing at the corticospinal tract decussation and optic chiasm (Yokoyama et al., 2001; Kullander et al., 2001; Lee et al., 2008). In the spinal cord, EphrinB3 is expressed by floor plate cells and its receptor EphB types are expressed on the axon surface of commissural neurons (Kadison, 2006). Unlike Netrin and Slit, Ephrin is a cell surface ligand, and its reaction with its receptor Eph requires direct cell-cell contact between the guided axons and the guidance signal cells (Kadison, 2006). Upon interaction, EphB expressing axons are repelled from the floor plate, which plays an important role in the crossing stage of spinal commissure formation (Yokoyama et al., 2001; Kadison, 2006). Mutation of either EphB or EphrinB3 cause increased recrossing, suggesting weakened repulsion (Kadison, 2006). Moreover, upon ligand-receptor combination, both Eph and Ephrin can trigger downstream reactions, which distinct the Ephrin-Eph reaction as bidirectional that may cause subsequent changes in both cell populations (Cowan and Henkemeyer, 2001; Xu and Henkemeyer, 2009).

In addition to the pairs described above, many other ligand-receptor pairs are involved in spinal axon pathfinding. Different receptors may interact with each other to change the

responsiveness to their ligands. On top of that, subtypes of ligands and receptors exist, which may have different binding affinity to their targets, or trigger different downstream cascades that result in different effects. Our understanding of CPG network formation is quite limited due to such complexity. In decades, insights of CPG network formation were drawn by comparing different mutant animals, but due to the effectiveness of different mutation methods used, the conclusions are often conflicting. Structural biology helps to explain ligand-receptor interaction and downstream effects on a molecular level. It can be predicted that the achievement of a more detailed understanding of the axon pathfinding and CPG formation will require the collaborative researches in structural biology, cell biology and neuroscience for a considerable amount of time still in the future.

In this study, we will try to study CPG formation by looking at two particular molecules: DCC and Nck2. By analyzing the locomotion characteristics in these DCC deficient and Nck2 KO mice, we try to understand the function of these two proteins in CPG formation, and discuss whether they are related to each other. We will first introduce their molecular structure, binding partners, expression patterns and known functions in locomotion in the following sections.

1.3 DCC

DCC, deleted in colorectal cancer, encoded by DCC gene, is a single transmembrane receptor protein in the immunoglobulin super family (IgSF, Keino-Masu et al., 1996). It shares a similar structure to its homologues, Frazzled in Drosophila, UNC40 in C.elegans, and neurogenin in vertebrates (Kolodziej et al., 1996; Chan et al., 1996; Meyerhardt et al.,

1997). It is initially believed to be a tumor suppressor due to the fact that it is constitutively expressed but silenced in tumors, and was therefore investigated for its controversial role in cancer development (Castets et al. 2011). Its role in axon guidance, mainly carried out by its combination to its ligand Netrin-1, is also studied. It is later found out that the binding of DCC and Netrin-1 can cause the axons to be either attracted or repelled from the source depending on the types of receptors expressed on the axon surface, which indicates DCC's bi-functional role in axon guidance and as a molecular switch (Hong et al., 1999; Finci et al., 2014). Understanding of the molecular structures of DCC, Netrin-1 and UNC5 (another receptor of Netrin-1) is the key to understanding their interaction and how this bifunctionality is achieved.

1.3.1 Molecular Structure of DCC, UNC5 and Their Ligand Netrin-1

DCC protein is typically composed of four Ig-like domains (Ig1-4) at the N-terminus, six fibronectin type III domains (FN1-6), a membrane proximal stalk and transmembrane segment, and a large cytoplasmic tail composed of about 350 residues including three interspecies conserved motifs (P1-3, Kolodziej et al., 1996; Figure 3B).

UNC5 gene was initially found in C. elegans and involved in axon guidance (Hong et al., 1999). Its protein product is a transmembrane receptor composed of 919 residues. Structurally, it has two Ig-like domains at the N-terminus, which is followed by two thrombospondin type 1 domains, and a large 550-residue intracellular segment, in which a DCC-binding domain (UPA) exists (Leung-Hagesteijn et al., 1992; Figure 3C). UNC5's vertebrate homologue is a receptor to Netrin-1 (Hong et al., 1999). Contrary to DCC, the

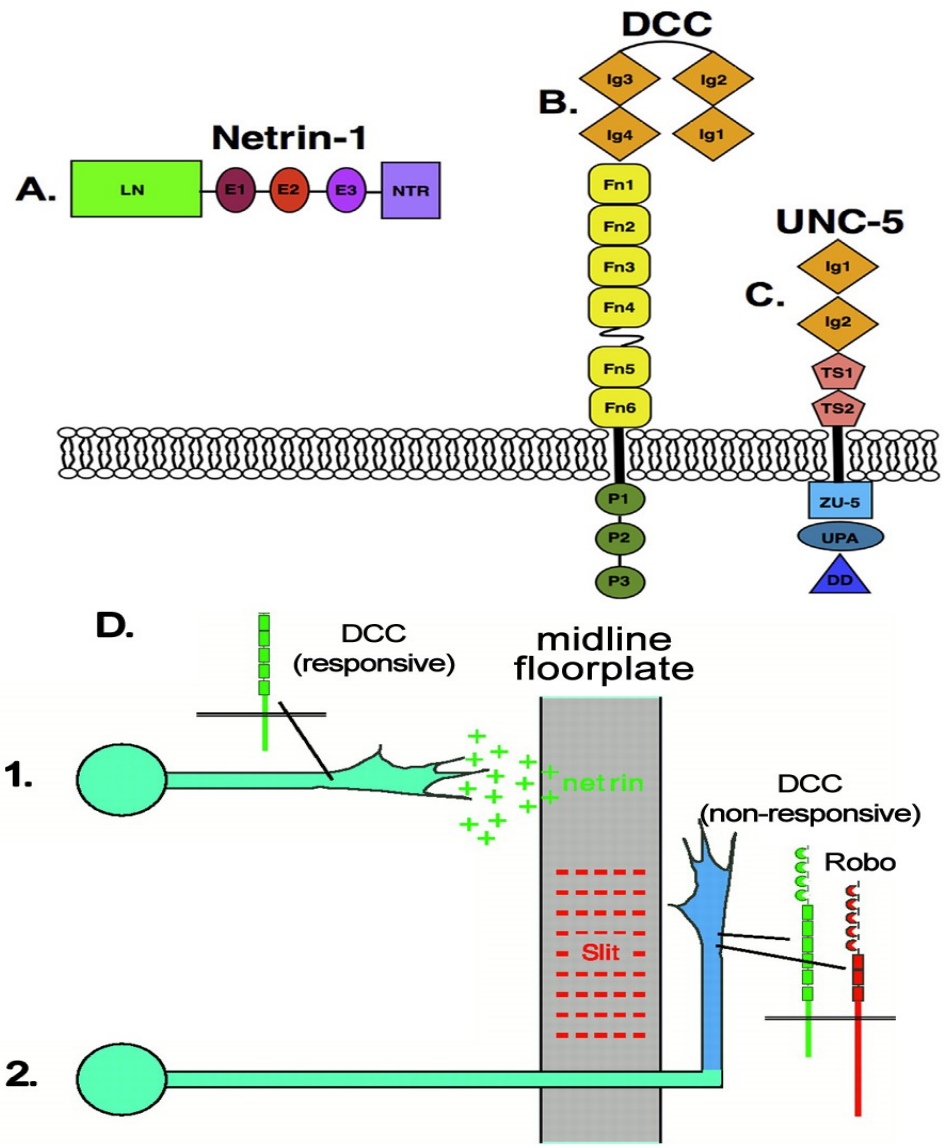

Figure 3. DCC Domain Architecture and Schemetic Function in Axon Pathfinding

The domain architecture of DCC ligand netrin-1 (A), DCC (B), UNC5 (C), and their orientation in relation to the plasma membrane. Adapted from Finci et al., 2015. Simplified process of commissure neuron axon pathfinding across the midline (D). Commissure neuron growth cones expressing DCC are attracted to the midline (floorplate) by secreted netrin (1). After the axon crosses the midline, the DCC receptrors on its membrane lost responsiveness to netrin, while another responsive receptor Robo interacts with its secreted ligand slit, resulting in the axon being repelled from the midline and thus the crossing.

binding of UNC5 to Netrin-1 cause the axons to be repulsed from the guidance molecule source (Leonardo et al., 1997).

Netrin-1 is a member of the netrin family and a ligand of DCC. It has a liminin-like domain (LN) at its N-terminus, which is followed by three EGF repeats (E1-3), and then a netrin-like domain at its C-terminus (Kennedy et al., 1994; Serafini et al., 1994; Figure 3A).

1.3.2 DCC as A Molecular Switch for Netrin-mediated Bifunctional Axon Guidance

Studies in structural biology indicate that there are two DCC-binding sites on netrin-1 that are functionally distinct from each other (Finci et al., 2014; reviewed by Finci et al., 2015). Site 1 is exclusively composed of E3 domain, and will bind to the FN5 domain of DCC. Site 2 is composed of E1 and E2 domains of netrin-1, and binds to a different portion of FN5 as well as part of the FN6 domain on DCC. The two binding sites also have different selectivity about their binding targets. Binding site 1 on netrin-1 is highly selective and specifically binds to DCC, while binding at site 2 involves very little direct interaction between the two proteins. Binding site 2 will bind to either DCC or other receptor molecule such as UNC5. As a result of such binding site characteristics, it can be depicted that netrin-1 can have two binding situations. It can either bind to two DCC proteins at both its binding sites, or else bind to 1 DCC protein at binding site 1 and 1 UNC5 protein at binding site 2.

It is important to notice that neither the intracellular domain of DCC or of UNC5 fold into defined 3D structure (Finci et al., 2014). When a single netrin-1 simultaneously binds to

two DCC proteins, it brings the two DCC molecules very close to one another with a cell surface distance as small as 20Å (Finci et al., 2014). Such small distance result in the homodimerization of the two DCC molecules by binding at the intracellular P3 motif, and further signaling is carried out which results in the chemoattraction (Finci et al., 2014). Similarly, when DCC and UNC5 are brought close to each other by netrin-1's binding to one of each, heterodimerization between the two occurs where P1 motif on DCC binds to the cytoplasmic DCC-binding domain (UPA) of UNC5, enabling downstream signaling that result in chemorepulsion (Finci et al., 2014). Thus, chemoattraction happens when netrin-1 binds only to DCC, while chemorepulsion happens when netrin-1 binds to both DCC and UNC5 in a UNC5 enriched environment.

It should be noted that DCC is essential in the repulsive effect resulting from UNC5's binding to netrin-1, since binding site 1 on netrin-1 specifically binds to DCC, and the DCC-UNC5 heterodimer formation is essential for downstream signaling pathways. Indeed, in vitro studies have proved that axons expressing UNC5 alone cannot be repelled by netrin (Hong et al.,1999; Finci et al., 2014). Therefore, DCC is a molecular switch in netrin-mediated axon pathfinding.

1.3.3 DCC as Dependence Receptor

Recent studies have indicated DCC's role as a dependence receptor (Mehlen and Furne, 2005), which means that depending on the availability of its ligand netrin-1, it can either inhibit or facilitate cellular apoptosis (Bredesen et al., 2005). DCC mediates axon guidance when netrin-1 is present, but will start apoptotic signal by activating caspase-3 during prolonged absence of netrin-1(Arakawa, 2004). It has been proved that DCC elicit

its tumor suppression effect through its triggering of apoptosis in a variety of tumor cells (Goldschneider and Mehlen, 2010; Castets et al., 2012; Krimpenfort et al., 2012). Although DCC's role as a dependence receptor is mostly described in tumor development, it is possible that this may also be functional in spinal cord development and neural progenitor fate decision.

1.3.4 Other Binding Targets of DCC and the Potential Implication

In addition to netrin1, other binding targets of DCC also exist and play roles in axon guidance as indicated by evidence in both in vitro and in vivo studies. Cerebellin 4 (CBLN4), a member of the C1q-tumor necrosis factor family, specifically binds to DCC at its FN4-FN5-FN6 region and competes with netrin-1 (Haddick et al., 2014). Dorsal repulsive axon guidance protein (Draxin), a 349-residue diffusible guidance signal molecule, preferentially binds to DCC at its N-terminal, which is different from netrin-1 binding site, and has a even higher binding affinity than netrin-1 in transfected cells (Islam et al., 2009; Ahmed et al., 2011). Draxin also binds to other netrin-1 receptors such as UNC5 and neogenin (Islam et al., 2009). DCC has also been shown to regulate axon pathfinding by modulating other pairs of signaling-receptor molecules. In vitro studies show that intracellularly, DCC can molecularly interact via its P3 domain with Robo at its CC1 domain (Stein and Tessier-Lavigne 2001; Yu et al. 2002). Such DCC-Robo interaction has been shown to affect corpus callosum formation in the brain through its regulation of Slit-mediated repulsion (Fothergill et al., 2013).

DCC's ability to interact with multiple targets certainly brings more complication in the already complex axon pathfinding signaling network.

1.3.5 DCC Expression in the Nervous System

Earlier studies have shown that DCC expression is restricted to the central nervous system (CNS) during rodent embryonic development. Gad and colleagues gave a detailed description about the spatial and temporal change of DCC during mouse embryonic development. They found that DCC has ubiquitous expression in CNS during earlier development, but by E18.5 is restricted to olfactory bulb, hippocampus and cerebellum, which all have sustained neurogenesis into postnatal life. More specifically, BrdU studies revealed that DCC has strong expression in the earliest post-mitotic neurons in both developing brain and spinal cord, but their expression is generally regardless of neuronal subtype (Gad et al., 1997).

Two indications can be drawn from the above results. Firstly, DCC expression in CNS is spatially and temporally correlated with neurogenesis. Secondly, its expression in neurons just entering postmitotic phase strongly suggests DCC's very important role in axon path finding and cell migration in almost all CNS neurons. Indeed, systemic loss of functional DCC results in defects in commissure formation in both spinal cord and brain. More specifically, these mice exhibit absence of corpus callosum and hippocampal commissure and severely reduced anterior commissure, as well as major defects in spinal cord commissural axon extension at all levels (Fazeli et al.,1997).

1.3.6 Current Understanding of DCC's Function in Locomotion

DCC mutation has been related in several studies to congenital mirror movement disorder (MM) in humans, which is characterized by unintentional mirroring in the homologous

motor systems on the opposite side during voluntary movements, more often in the distal upper limbs (Srour et al., 2009; Depienne et al., 2011; Meneret et al., 2014; Franz et al., 2015). DCC's is believed to affect corticospinal tract formation as MM patients exhibit abnormal ipsilateral corticospinal pathways (Srour et al., 2009). More specifically, the mutation lies in the extracellular domain of DCC which made it unable to bind to netrin (Srour et al., 2010). However, the result remains inconclusive due to the genetical heterogenerosity of MM patients (Depienne et al., 2011).

The majority of the studies in DCC function in locomotion put emphasis on its role in commissure formation. The Kullander lab presented two studies about the function of Netrin 1 and DCC in CPG and locomotion. In the study by Rabe and colleagues, Netrin-1 mutant mice spinal cords show strict left-right synchronization at both L2 and L5 during drug induced fictive locomotion, but normal alternation between ipsilateral L2/L5 is preserved (Rabe et al., 2009). Interestingly, when DCC is knocked out or mutated, spinal cords from these mice show a more severe coordination problem, specifically, bilateral ventral roots on the same lumbar level exhibit episodes of both synchronized and alternating firings that switch fast and irregularly (Bernhardt et al., 2012). The ipsilateral L2/L5 alternation is also preserved in DCC KOs, suggesting a functionally normal formation of flexor/extensor coordination. Neuronal tracing in both mutant animals show a vast reduction of inter- and intra-segmental commissure neurons. However, immunohistochemical staining show that although both excitatory and inhibitory commissure neurons are reduced in numbers, Netrin-1 mutation preferentially reduce inhibitory neurons, causing an increased excitatory/inhibitory ratio among the remaining commissure neurons. In contrast, DCC mutation reduces both excitatory and inhibitory

interneurons at similar rates, resulting in the excitatory/inhibitory ratio of the remaining populations to be not significantly different from that in the controls. Since inhibitory commissure input is majorly responsible for the left-right alternation circuit and excitatory commissure input is responsible for left-right synchronization circuit, the group proposed that the relatively increased excitatory input in Netrin-1 mutants is the reason for its strict synchronization in left-right coordination, while the reduction in both excitatory and inhibitory input in the DCC KOs results in the animals' uncoordinated movements. This notion is supported by the group's further discovery that the most ventrally located Nkx2.2 expressing V3 population, which is believed to be mostly excitatory, is not affected by the loss of Netrin-1 but is reduced when DCC is deficient. The pharmacological strengthening of inhibitory input by adding glycine reuptake inhibitor sarcosine and GABA reuptake inhibitor nipecotic acid (NA) during fictive locomotion is not able to restore the loss of asynchronization in the Netrin-1 deficient spinal cords.

The above studies from the Kullander lab provide an insight into Netrin-DCC function in CPG formation. However, since both Netrin1 and DCC deficiency have lethal effect around birth, locomotion in adults cannot be described in these animals. Moreover, since both Netrin1 and DCC are expressed in many regions throughout the nervous system aside from lower spinal cord, the phenotype described in these studies could be mixed results from deficiency in local lumbar CPG and deficiency in higher levels. Therefore, a different mutation system is needed to enable the locomotion analysis in adult animals, as well as to look in more detail into the potential multiple functions of DCC on locomotion carried out by its expression in different positions.

1.4 Nck

The Nck genes are a family of evolutionally conserved genes originally isolated from human melanoma cDNA library (Lehmann, Riethmuller and Johnson, 1990). In humans and rodents, two members of this gene family, Nck1 and Nck2, encode two cytoplasm located adaptor proteins that transduce signals from receptor tyrosine kinases to downstream recipients (Chen et al., 1998; Frese et al., 2006).

1.4.1 Molecular Structure of Nck

Nck1 and Nck2 proteins are 48 kilodaltons molecules that share a common structure: both contain three Src-homology 3 (SH3) domains at N-terminus and one Src-homology 2 (SH2) domain at C-terminus, with small spacer regions linking in between (Lettau et al., 2009). The individual SH2 and SH3 domains in Nck1 and Nck2 show very high level of homology, while major amino acid sequence difference between the two exist in their spacer regions, which together result in a 68% amino acid similarity between the two proteins (Li, 2001; Chen et al., 1998; Figure 4A).

1.4.1.1 SH3 Domains

The SH3 domains of the Nck proteins bind to the consensus sequence PXXP (P = proline, X = any amino acid; Ren et al., 1993). However, due to the three-dimensional structure of the molecule, the three SH3 domain show different affinity to target proteins based on their location (Wunderlich, 1999). Thus, the three SH3 domains may bind to different targets. Moreover, three SH3 domains function collaboratively to increase the selectivity of Nck proteins' binding to their partners as a result of multiple low affinity interactions

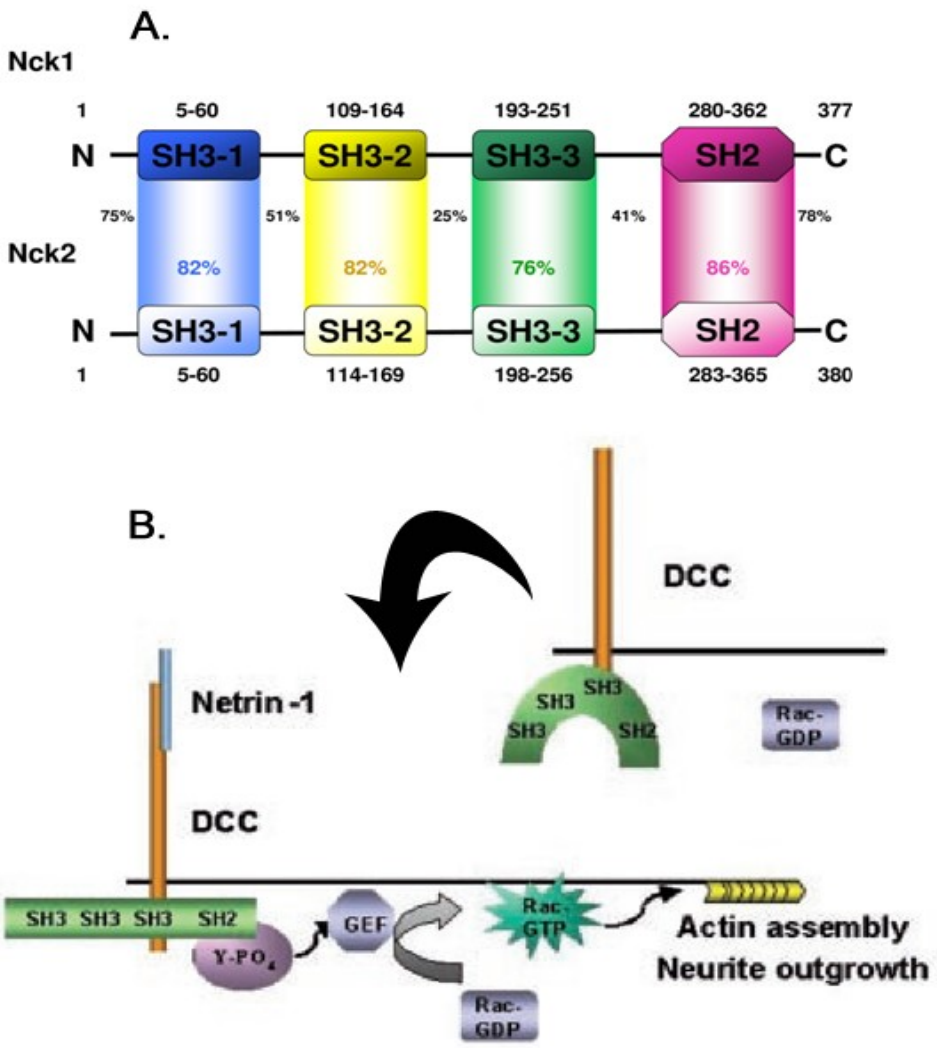

Figure 4. Nck Domain Architecture and Interaction with DCC

Schematic illustration of human Nck1 and Nck2 protein domain architecture (A). Nck protein contain three SH3 domains and 1 SH2 domain. Numbers on top and bottom panel indicate amino residue position of each domain. Numbers in the middle indicate the percentage of homology between each domain and linking area in Nck1 and Nck2. Adapted from Lettau et al. 2009. Schematic illustration of Nck1 interaction with DCC (B). Nck1 binds to intracellular DCC via the third SH3 domain. Netrin-1 binding to extracellular DCC trigures the recruitment of molecules like GEF and Rac, and results in downstream reaction like actin assembly or neurite outgrowth. Adapted from Li et al., 2012.

(Alder et al, 2000; Wunderlich, 1999). Most cell surface receptors that interact with Nck at SH3 domains are related in cytoskeleton formation and axon guidance.

1.4.1.2 SH2 Domains

The SH2 domains in Nck proteins binds to the phosphorylated tyrosine (pY) residues (Ren et al., 1993; Pawson, 2001), which is later proved to be the consensus sequence YDXV (Y = tyrosine, D = aspartic acid, X = any amino acid, V = valine; Blasutig et al., 2008). The structure of the SH2 domain includes a positively charged pocket that selectively binds to the phosphorylated tyrosine (Pawson et al., 2001). The SH2 domain in Nck also usually binds to cell surface receptors, since these tyrosine kinase containing receptors become phosphorylated upon interaction with their respective ligand, which will recruit SH2 domain containing molecules (Li et al, 2001).

1.4.2 Binding Targets of Nck Proteins

The Nck proteins can bind to a lot of receptors via both either SH2 or SH3 domains, which is the reason why they play multiple roles in different biological processes including cancer progression, cytoskeleton regulation and axon guidance, T-cell receptor signaling and translational control (Adler et al., 2000; Li, Fan and Woodley, 2001; Bladt et al., 2003; Jones et al., 2006). In developing neurons, Nck is intracellularly recruited by many axon guidance ligand or receptor molecules, including Robo, Ephrin B type, Eph and DCC (Li, 2002; Round and Sun, 2011; Mohamed et al., 2012). The binding of Nck is essential for the trigger of downstream reactions upon ligand-receptor interaction (Stein et al., 1998). In this section, we will introduce some binding partners of Nck that are involved in axon guidance and neuronal development.

1.4.2.1 Robo

In drosophila, Nck's homologue dock is coexpressed with Robo in the longitudinal axons of the developing nervous system (Fan et al., 2003). Upon robo's extracellular binding with slit, the first and second SH3 domains of dock molecularly interact with the CC2 and CC3 proline rich regions of robo (Fan et al., 2003). Consequently, slit-robo-dock complex recruits pak, which activates RAC1 activity, as well as guanine nucleotide exchange factor (GEF), thus regulates actin cytoskeleton formation (Fan et al., 2003; Yang and Bashaw, 2006).

Similar to that in drosophila, it is later found in vertebrates that both Nck proteins bind to Robo1 and Robo2 via atypical SH3-mediated mechanism that requires multiple SH3 domains (Wunderlich, 1999). However, only loss of Nck2 can abolish the slit-Robo mediated cortical axon elongation and dentrite branching in vitro, indicating its specific role in slit-induced cytoskeleton rearrangement that regulates neuronal morphology (Round and Sun. 2011). The significance of these studies is debated as in vivo experiments are still lacking, thus not determining Nck's function in regulating slit-robo signal in spinal cord development.

1.4.2.2 Ephrin B and Eph

As already described above, Ephrin B 1-3 ligands regulates midline crossing in embryonic spinal cord by eliciting repulsion upon combination to its receptor eph expressed on the opposing cell (Kullander et al., 2001; Yokoyama, 2001; Kadison, 2006). This regulation requires direct cell-cell interaction, and the effect is bidirectional. Nck

adaptor proteins are involved in the downstream pathways of both Ephrin B ligands and eph receptors. Nck2, via its SH3 domains (Cowan and Henkemeyer, 2001), binds to the pY residue 298 of Ephrin B1 or the pY 304 residue of Ephrin B2 (Bong et al., 2004), and consequently initiate intracellular actin regulation. Interestingly, such interaction is not found between Ephrin B and Nck1 (Bong et al., 2004). Nck2 also reacts with Ephrin B3 via its 2nd SH3 domain upon eph receptor binding and recruits dock180 and PAK thus regulate axon pathfinding in hippocampal neurons (Xu et al., 2009, Xu et al., 2011). The interaction between Nck2 and Ephrin B3 may be of great importance in regulating the development of spinal locomotor circuits, as described below in 1.4.5. It is important to understand that although no evidence suggests the interaction between Nck1 and the Ephrin B ligands, their interaction is still possible due to the highly conserved SH2 and SH3 domains between Nck1 and Nck2, and may play some role in vivo. On the other hand, the different interaction pattern with the Ephrin B ligands between the two Nck proteins may bring diversity in development and network formation.

Ncks also interact with ephrin receptors EphA2/3/4 and EphB1/2 via intracellular phosphotyrosine residues (Holland et al., 1997, Stein et al., 1998; Hock et al., 1998; Bisson et al., 2007; Mohamed et al, 2012). Nck was proved important in the development of EphA4 expressing corticospinal tract neurons, and loss of Nck leads to these neurons' recrossing the midline (Fawcett et al., 2007). Thus, Nck's interaction with Eph receptors may affect locomotion at a higher level.

1.4.2.3 DCC

The interaction between Nck and DCC pathway has also been described by several studies. Nck1 interacts with DCC via first and third SH3 domain upon Netrin1 binding, and recruits PAK which is essential to induce RAC1 activity (Li, 2002; Shekarabi, 2005). More specifically, netrin binding to DCC recruits many molecules intracellularly, including PAK kinase, Nck, TRIO GEF, CDC42, RAC1, WASP, SRC and FYN kinases, and together they form a complex (Figure 4B). Nck acts as a bridge between the interaction of TRIO/PAK and DCC, and is essential for complex formation (Briancon-Marjollet et al., 2008, Ren et al., 2004; Li et al., 2004). Nck may also bridge the interaction of PAK and WASP to DCC as proposed by some group (Shekarabi et al., 2005). Both Nck1 and Nck2 are shown to interact with DCC and can be involved in the transduction of DCC signals. However, the physiological significance in locomotor circuit development is not described in detail, and the potential distinct function of Nck1 and Nck2 in such situation is yet to be studied.

1.4.3 The Redundant and Distinct Function of Nck1 and Nck2

Because of the sequence identity of their SH2 and SH3 domains, it is natural to assume that the two proteins share a lot of common binding targets. Functional redundancy between the two Nck proteins has been proved in many physiological environments by multiple groups (Frese et al., 2006; Fawcett et al., 2007; Jones et al., 2006; Bladt et al., 2003; Chen et al., 1998).

On the other hand, several studies do show that some structural difference exist between the SH2 and SH3 domains in the two Nck proteins (Arold et al., 1998; Kaneko et al., 2010; Chen et al., 1998), which indicates the potential different roles Nck1 and Nck2 play

in vivo. This notion has been supported by several in vitro studies. Only Nck1 constitutively binds to DCC (Li, 2002). NCK2, but not NCK1 binds to the Ephrin B receptors and induce the reverse signaling upon extracellular interaction with Eph (Cowan and Henkemeyer, 2001; Bong et al., 2004). Only Nck2 via its SH2 domain binds to Dab1, a docking protein phosphorylated by Reelin, which also regulates actin cytoskeleton remodeling (Pramatarova et al., 2003). Only Nck2 is essential in Robo induced neurite outgrowth (Round et al., 2010). The distinct function of Nck1 and Nck2 in vivo, however, remains elusive.

1.4.4 Nck Protein Expression in the Nervous System

The different expression pattern of Nck1 and Nck2 in the developing mice nervous system has been described by Lane and colleagues. In E11.5 mice, Nck1 has widespread expression in the ventral, medial spinal cord, and also has lower level in the dorsal medial region. At P5, Nck1 is universally expressed in all spinal regions. On the contrary, NCK2 shows more localized expression at midline and floor plate and lower expression in the immature motor neurons at E11.5, but has high expression in midline and motor neurons and very low expression in interneurons at P5 (Lane, Qi and Fawcett, 2015). Such difference in expression pattern further suggests the distinct roles the two Nck proteins play in spinal cord development.

1.4.5 Current Understanding of Nck's Function in Locomotion

In earlier studies, Fawcett and colleagues discovered that Nck depletion in the nervous system cause mice to have a hopping gait (Fawcett et al., 2007). The hopping gait was believed to be caused by defects in both cortical spinal tracts (CST) and local lumbar

CPG, since anatomically the mice show reductions of both dorsal faniculus (DF) and posterior tract of anterior commissure sizes. Malformation of the lumbar CPG in these mice is further supported by the early appearance of hopping gait before CST innervations. Since the mutation of Ephrine-B3, EphA4 or α-chimaerin all result in hopping mice with anatomical defects similar to Nck deficient mice, Fawcett and colleagues proposed that the Nck elicits its effect on locomotion via in a pathway related to EphA4 and α-chimaerin, as their interaction is proven in vitro. The disruption of axon guidance is proposed to be the cause of locomotion defects in these animals.

The relationship between Nck and DCC in the sense of locomotion has also been discussed in several studies. Phenotypically, the loss of asynchronization in DCC KO mice and Netrin1 mutant mice during locomotion is comparable to that in the Nck deficient mice. The in vivo relationship of DCC and Nck in the developing spinal cord has also been described. In the study by Lane and colleagues, the expression of Nck proteins were essential to the normal axon outgrowth and growth cone morphology in DCC positive neurons in vitro, and Nck deficiency in vivo caused defasiculation of DCC positive axons as well as their failure to project to the floor plate and across the midline (Lane, Qi and Fawcett, 2015).

Despite the similarity of behavioral and anatomical changes between Nck deficient mice and mice with mutation of Nck's binding targets, it is not clear which population of neurons are affected. In ephrin-B3 and EphA4 mutant mice, the synchronized motor neuron firing at L5 level in fictive locomotion can be rescued by the application of glycine uptake inhibitor sarcosine, which restore the alternating firing completely

(Kullander, 2003). It is therefore believed that in these mice, excitatory input into the contralateral side is increased by the abnormal commissural formation, and the application of sarcosine increases the inhibition drive in the CPG, thus reverting the loss of asynchronization (Kullander, 2003). In Nck deficient mice, the application of sarcosine can shift the bilateral coupling value away from 0, but was unable to restore it to normal alternation like it did in the ephrin-B3 and EphA4 mice (Kullander, 2003; Fawcett, 2007). This supports the idea that Nck may exert its effect on locomotion via multiple pathways. In addition to its binding to EphA4 and ephrin-B3, Nck's binding to other targets like DCC and Robo may also alter the formation of local CPG and result in altered locomotion pattern. In support of this notion, it is found that EphA4 positive neurons in the spinal cord can be either excitataory or inhibitory (Butt et al., 2005; Lundfald et al., 2007), which could be a result of Nck's interaction with DCC or Robo in a subpopulation of EphA4 positive neurons where DCC or Robo is coexpressed. The interaction between Nck and the above target molecules may also exist in EphA4 negative populations and be involved in the fate decision, thus affecting CPG formation.

The functional redundancy of Nck1 and Nck2 is indicated in the above studies, as single mutation or deletion of Nck1 or Nck2 cause minimal effect behaviorally or anatomically. However, very few studies have focused on the potential distinct function of the two Nck proteins, and analyze the locomotion phenotype of Nck single knockout mice in detail.

1.5 Rationale and Specific Objectives

Rhythmic locomotion requires the structural integrity of CPG. CPG formation during development involves the generation, differenciation and connection of many different

types of interneurons. The development and migration of interneurons need the spatially and temporally correct activation of many molecular reaction and downstream pathways. DCC, a receptor for chemoattractant netrin-1, is important in spinal ventral commissure formation. Loss of DCC results in reduction of both excitatory and inhibitory commissure input in CPG and uncoordinated left-right alternation during locomotion. Loss of DCC's ligand Netrin-1 leads to preferential reduction of inhibitory commissure input in the CPG and left-right synchronization during locomotion. Loss of Nck also results in left-right synchronization that is likely caused by reduced inhibitory input. Since locomotion in adult DCC dificient or Nck2 KO animals hasn't been described, the distinct role of Nck1 and Nck2 in locomotion isn't clear, and the relationship of Nck2 and DCC in locomotion hasn't been studied intensively, the following hypothesis and objectives are established:

Hypothesis: *The adaptor protein Nck2 plays a role in locomotor network formation, which partially acts via a DCC-independent pathway.*

Objectives:

1) Identify the phenotype of adult DCC deficient mice during treadmill locomotion.

2) Identify the phenotype of adult Nck2 KO mice during treadmill locomotion.

3) Compare the locomotion of DCC deficient and Nck2 KO mice and examine the relationship of DCC and Nck in locomotion, and Nck2's potential distinct role.

CHAPTER 2 MATERIALS AND METHODS

2.1 Mice

Mice are kept and all procedures were performed in accordance with the Canadian Council on Animal Care and approved by the University Committee on Laboratory Animals at Dalhousie University.

2.1.1 DCC Mice Strains

5 mouse strains provided by Dr.Charron Frédéric, Institut de recherches cliniques de Montréal (IRCM) are used in this study. 1) Hoxb8::Cre$^{+/-}$;Tom$^{+/-}$;DCC$^{f/f}$; 2) Hoxb8::Cre$^{+/-}$;DCC$^{f/-}$; 3) Hoxb8::Cre$^{+/-}$;DCC$^{f/+}$; 4) Hoxb8::Cre$^{-/-}$;DCC$^{f/-}$; 5) Hoxb8::Cre$^{-/-}$;Tom$^{+/-}$;DCC$^{f/f}$. These mice are generated using Hoxb8::cre mice described before (Witschi et al., 2010). Homeobox gene Hoxb8 is used as promoter for Cre expression to restrain the elimination of the floxed DCC to the level below C2 in the spinal cord. Strains 1) and 2) are used as DCC deficient group; strains 3) and 4) are used as DCC heterozygous group; strain 5) is used as control group. All tests are performed on mice of both genders at the age of two months old.

2.1.2 Nck2 Mice Strains

3 mouse strains provided by Dr. James P. Fawcett are used in this study. Nck2$^{-/-}$ mice are used as Nck2 straight knockout group; Nck2$^{+/-}$ mice are used as Nck2 heterozygous group; Nck1$^{+/-}$;Nck2 $^{f/f}$ mice are used as the control group. Generation and maintenance of the strains have been previously described (Bladt et al., 2003). All tests are performed on mice of both genders within the age range of 2.5-6 months old.

2.2 Treadmill Locomotion

2.2.1 Two Treadmill Systems

2 treadmill systems are used in the study.

System 1 is a treadmill (Cleversys, Inc.) equipped with a transparent belt and a high speed camera (Basler) underneath. Mice were put in a 161.1cm^2 chamber during recording. Videos are taken from below the belt at the rate of 90 fps using supplied software BCam Capture Version 2.00 (Cleversys, Inc.) and analyzed using supplied software Treadscan 4.0. System 1 is used for interlimb coupling and step cycle analysis.

System 2 is a custom made treadmill system previously described (Pearson et al., 2005). Mice are placed in an enclosure above the treadmill belt (21 cm long, 5 cm wide) during recording. Videos are taken from the side of the treadmill with a high speed camera (FASTEC IMAGING) set at the rate of 250 fps, and later analyzed with Motus 9 motion analysis system (VICON). System 2 is used for joint angle, step cycle and EMG analysis.

2.2.2 Locomotion on Treadmill under Set Speed

All mice are trained once on the respective treadmill system 1-2 days prior to the behavioral tests. During the training session, mice are put into the chamber on the treadmill and allowed to explore for two minutes. Treadmill is then turned on and set at 1cm/s for the mice to get used to, then gradually increasing speed to 10cm/s and kept constant at that level. The rate of the speed increase varies according to each mouse's adaptation capacity. The total length of locomotion on treadmill is two minutes.

Mice are tested on the treadmill under the set speeds of 8, 15, 25, 35, 45, 55, 60 and 65cm/s. Each mouse performs two 15s trials at each speed in an increasing order, and is allowed a three minute rest between each trial. An additional trial is performed if a mouse shows difficulty catching up with the set speed. If the mouse still cannot catch up with this speed, the rest speed sequence is not tested on this specific mouse. The experiment is carried out on each mouse three times with three days in between each test.

2.2.3 Maximum Locomotion Speed

Maximum treadmill locomotion speed of each mouse is recorded using the following two methods.

1) Within the sequence of 8, 15, 25, 35, 45, 55, 60 and 65cm/s, the maximum set speed of the treadmill a mouse can reach in the chamber of treadmill system A is recorded as its max set speed. three chances are given to each mouse on three respective days with three days in between each test to eliminate the factor of bad performance.

2) The chamber in treadmill system A is removed and the mouse is given the total space of the treadmill. Treadmill speed is gradually increased from 15cm/s to the highest a mouse can reach as it is running. This highest speed shown on the treadmill system is recorded as max speed of this individual mouse. three chances are given to each mouse on three respective days with three days in between each test to eliminate the factor of bad performance.

2.3 Interlimb Coupling Analysis

Videos taken from below treadmill system A for each trial are clipped, and clips showing typical locomotion under the set speeds for a minimum of 20 consecutive steps are imported and analyzed using Treadscan 4.0. Settings for analysis of each trial varies according to the color and body shape of the mice, but are adjusted according to the principle for most accurate paw detection. The result of each trial is exported into Excel and further analyzed within and between genetic groups.

3 sets of interlimb coupling data analyzed are: 1) Forelimb homologous coupling; 2) Hindlimb homologous coupling; 3) Diagonal coupling (Figure 5). For homologous coupling, data using both left side and right side as reference limb are used and combined for analysis. For diagonal coupling, only data using front limbs as reference limbs are used and combined for analysis. Each coupling value is automatically given by Treadscan calculated from the time points when the reference foot or investigated foot touches the ground. Coupling values range from 0 to 0.5, with a value closer to 0 indicating a more synchronized movement of the two limbs, while a value closer to 0.5 indicates a more alternative movement. The collective coupling data of one mouse under one speed is put into bins and generates a percentage based distribution, after which the distribution of different mice in one genetic group under that speed is put together to generate the distribution graph of that group using Matlab. The mean value of each mouse's coupling data is used in the t test for comparison between groups.

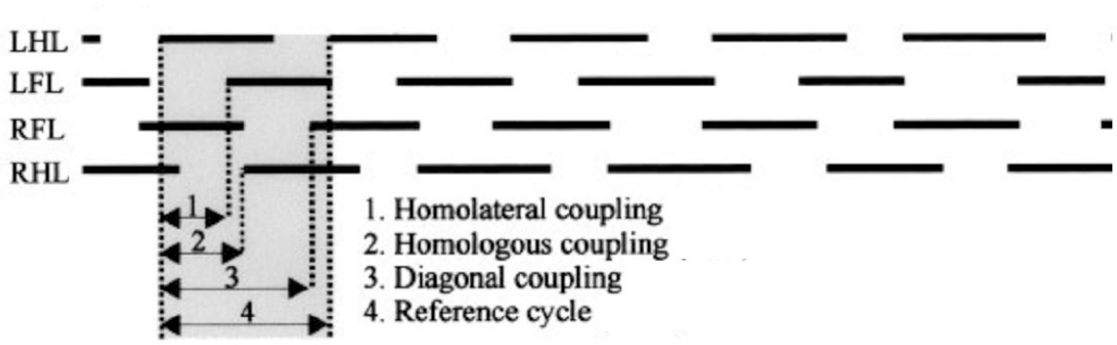

Figure 5. Interlimb Coupling Concept Demonstration

Step bar graph of the four limbs generated from videos of locomotion. Solid lines indicate stance; blanks between solid lines indicate swing. The concept of homolateral coupling, homologous coupling and diagonal coupling are indicated in the figure. Adapted from Leblond et al., 2003; LHL=left hindlimb; LFL=left forelimb; RFL=right forelimb; RHL=right hindlimb.

2.4 Normal Step Sequence

The time point of a foot contact the ground is marked as the stance onset of the particular foot. The sequence of the four consecutive stance onsets of a mouse's four feet is recorded as a step sequence. In each trial, the most appeared step sequence is recognized as the normal step sequence. The frequency of the appearance of the normal step sequence in all step sequences is calculated and given by Treadscan 4.0 as the percentage of normal step sequence, which is an indicator of step sequence uniformity.

2.5 Joint Angle Analysis

Mice were briefly anesthetized with isoflurane before testing, and three-dimensional reflective markers custom made from light reflective tape (3M 7610 Retroreflective Tape) were glued onto the shaved skin at crest, hip, ankle, paw joint and the lateral side of tip of the fourth toe with Krazyglue. Mice were allowed to wake up from anesthesia on system 2 treadmill and recover for approximately five minutes before trials. Videos taken from the side are imported and analyzed using Motus 9 motion analysis system. Positions of the crest, hip, ankle, paw and toe joints are directly recognized from the video. Since skin on the knee moves a lot during locomotion, position of the knee joint is calculated by measured femur and tibia length. Joint angle data is then calculated by Motus and then imported to Spike 2. Peaks and troughs of the hip, knee and ankle joint curves are automatically detected by Spike 2 and marked for joint cycle analysis, and used as reference points in joint angle graph generation using Matlab. The Matlab scripts used in joint angle graph generation and all other Matlab scripts for analysis purposes in this study are kindly provided by Mingwei Liu in our lab.

2.6 Step Cycle Analysis

The following five parameters are used in step cycle analysis. 1) stance duration: the time length of the foot in contact with the ground in one step (from the start of contact to the lift of foot); 2) swing duration: the time length of the foot in the air in one step (from the lift of foot to it contacts the ground); 3) stride duration: the time length of a single step (stance duration plus the consecutive swing duration); 4) stride length: the distance travelled in one stride; 5) stride frequency: the reciprocal of stride duration.

Data exported from Treadscan 4.0 are directly used for step cycle analysis. In the data exported from Motus, position of the toe is used as reference of step cycle. Specifically, the time that the toe x value reaches its maximum in a step is recognized as the start of stance, while the time of toe x value reaches its minimum is recognized as the end of the stance.

2.7 Joint Cycle Analysis

Joint angle curves with automatically detected peaks and troughs are exported from Spike 2 for joint cycle analysis in Excel.

In hip cycle analysis, the time point hip angle reaches its maximum in one step is marked as Hip-p, and Hip-t is when it reaches its minimum. The time length from Hip-p to Hip-t is referred to as hip flexor phase (Hip F), and from Hip-t to the next Hip-p is hip extensor phase (Hip E). The added time length of hip flexor phase and its consecutive extensor phase is one hip cycle.

In ankle cycle analysis, ankle angle curve has two peaks (Ankle-p1, Ankle-p2) and two troughs (Ankle-t1, Ankle-t2). The time length from Ankle-p1 to t1 is referred to as ankle flexor phase (Ankle F); from t1 to p2 as ankle extensor phase I (Ankle E1); from p2 to t2 as ankle extensor phase II(Ankle E2); and from t2 to next p1 as ankle extensor phase III (Ankle E3). Ankle F and its consecutive E1, E2 and E3 constitute one ankle cycle (Figure 10B).

2.8 Making of EMG Electrodes

6 channel EMG electrodes are custom made for EMG recording in the mice. The wires used in the electrode are 7-stranded with 0.14 mm outside diameter, Teflon coated annealed stainless steel wire (A-M systems, Catalog Number 793200). For muscles GS, TA and IP, paired electrodes are made by twisting two pieces of wire together and placing a knot at one end. 0.5mm of Telflon insulation was removed from each wire creating 1 bared region on each wire 1.5 mm away from each other. The ends of the two twisted wires are crimpled into a 27 ½ gauge needle for implantation. 10 cm of wires from the knot are left on the opposite ends and bared for soldering onto connector. The wires run parallel to muscle fiber when implanted. For muscle BF, electrodes are made in a similar way except that the paired wires are free from each other instead of twisted, and a 30 ½ gauge needle is used on each free end of the paired wires. This untwisted electrode is better for BF because of its relative thin but wide shape, and the two paired wires run independently but perpendicular to muscle fiber when implanted, with a distance about 2.5 mm in between. Depending on the muscles being investigated in each animal, six pairs of twisted/untwisted wires are soldered onto a six-pin miniature connector

(SamTech). Epoxy (Devcon 5 min Epoxy Gel) was applied onto the underside of the connectors for insulation.

2.9 EMG implantation

Mice are put on e-collars two days before surgery for adaptation. Analgesics (a mixture of ketamine 100mg/kg and buprenorphine 0.1mg/kg are given 30 minutes prior to surgery. E-collars are removed after isofluorene anesthetic induction and throughout surgery.

The procedure of EMG implantation surgery has been previously described (Pearson et al., 2005). Briefly, hair is removed around surgical site and skin is sterilized with germicidal soap, 70% ethanol and providone-iodine disinfectant. Cuts are made on skin to expose target muscles, and in the midline on the back of the mouse to implant the connector. The connector is buried on the back of the mouse under the skin with its posterior in line with the level of the mouse's crest, and the surrounding skin is sutured to stabilize the connector and ensure minimal exposure. Wires are placed comfortably under the skin and adipose tissue before reaching the target muscle. The wires from the electrode are drawn through the muscles by the attached needles, until the knot was firmly against the wire's entrance on the muscle, so that the bared part is safely buried in the muscle. Another knot was put at the wire's exit on the muscle and tightened to make sure the implanted part is stabilized. The wires are cut two mm from the knot at the exit and the needles are removed. The free end of the wires are put under the skin and stabilized before suture of the wound.

E-collars are put back on shortly after the removal of anesthesia and the mouse is allowed to wake up in its home cage on a heat pad. Mice are closely monitored for the consecutive week after the surgery for the recovery of its wounds and body weight. E-collars are removed when the wounds are properly recovered unless a dramatic body weight loss (>10% weight before surgery) is observed, in which case they will be removed immediately. Mice are allowed at least 1 week of recovery after surgery before they are tested on treadmill.

2.10 EMG Analysis

The following muscles are investigated unilaterally or bilaterally: hip flexor Iliopsoas (IP), hip extensor and knee flexor Bicep femoris (BF), ankle flexor Tibialis anterior (TA) and ankle extensor Gastrocuemius-soleus (GS). A 40 cm lightweight cable was connected to the connector of the implanted electrode during anaesthesia. EMG signals were amplified and captured with Spike 2 during treadmill locomotion, and later synchronized with joint angle data exported from the videos analyzed in Motus. EMG signals are normalized according to step cycle phase or ankle angle phase, and average EMG curves are drawn in Matlab.

CHAPTER 3 RESULTS

3.1 DCC Deficient Mice

3.1.1 DCC Deficient Mice Show More Synchronized Hindlimb Movement

We first investigated the locomotion pattern of DCC deficient and control mice on treadmills under a series of set speeds. Of the five strains of mice used in this study, the wildtype control mice $cDCC^{f/f}$ (Hoxb8::$cre^{-/-}$;$DCC^{f/f}$;$TdTomato^{+/-}$) display a walking gait at lower speeds of 8cm/s and 15cm/s, and gradually switch to a trotting gait when treadmill speed increases above 25cm/s. Trotting is maintained at all tested higher speeds. This gait change is comparable to the current standard description of mice gait change according to speed (Bellardita and Kiehn, 2015). Since speeds higher than 65cm/s cannot be achieved on our treadmill system, galloping and bouding gait that usually appears at speed higher than 85cm/s is not observed in our study. The observed gait change in the $cDCC^{f/f}$ mice results in their near 0.5 frontlimbs and hindlimbs homologous coupling value (Figure 6A, B, D), which came closer to 0.5 as the speed increases (Figure 7A-D, M-P, Table 1). The frontlimb/hindlimb diagonal coupling of the $cDCC^{f/f}$ mice is more synchronized as can be expected under a normal walking or trotting gait (Figure 6C). The interlimb coupling of the two DCC heterozygous groups $cDCC^{f/+}$ (cre+/-;DCCf/+) and $cDCC^{f/-}$ (cre-/-;DCCf/-) is not different from $cDCC^{f/f}$ mice. Both heterozygous groups also display alternating forelimbs and hindlimbs homologous coupling at all speeds, and their gaits become increasingly uniform trotting as speed increases (Figure 6E-L). In contrast, the two DCC deficient groups $mDCC^{f/f}$ (cre+/-;Tom+/-;DCCf/f) and $mDCC^{f/-}$ (cre+/-;DCCf/-) display a large proportion of synchronized hindlimb movements at all tested speeds (Figure 6M-T), which is even more dramatic at higher speeds (Figure 7E-L,

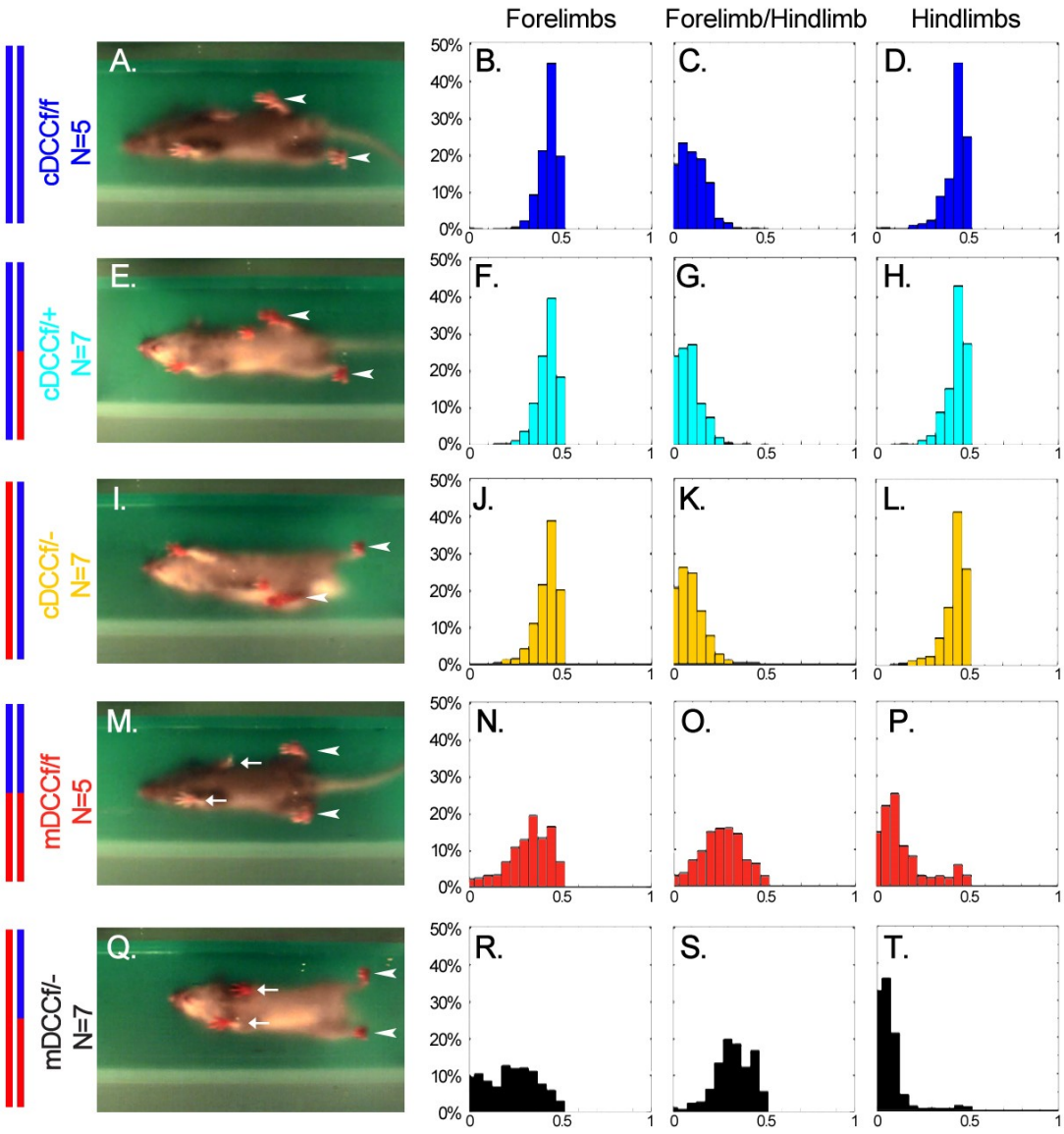

Figure 6. Ablation of DCC below thoracic level leads to a hopping gait.

At 25cm/s treadmill speed, control mice (A-D) and DCC heterozygous mice (E-L) display typical trotting gait in which both forelimbs and hindlimbs show alternating pattern while forelimb/hindlimb diagonal coupling show more synchronized movements. DCC deficient mice (M-T) show synchronized hindlimb movement and out of phase forelimb coupling at the same speed. Cre+;DCCf/- mice show a larger proportion of synchronized forelimb movement compared to Cre+;Tom+/-;DCCf/f mice (N,R). N=number of mice.

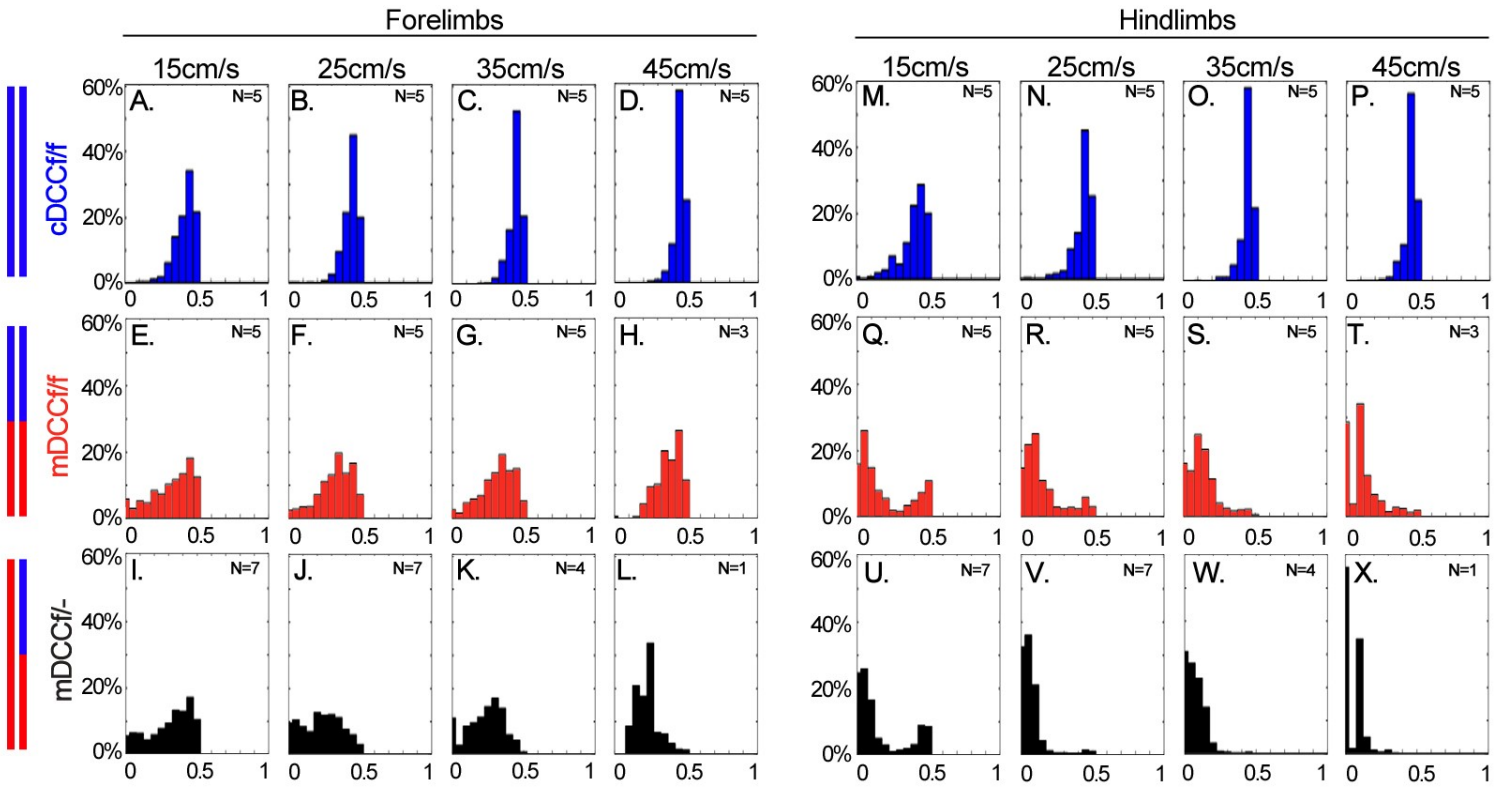

Figure 7. Homologous coupling at different speed.

Homologous coupling values of forelimbs and hindlimbs in control mice both shift closer to 0.5 as locomotion speed increases (A-D, M-O). Both DCC deficient groups show synchronized and alternating hindlimb movement at lower speed, but synchronization increases with speed(Q-X). Both DCC deficient groups show out of phase forelimbs coupling at all speeds (E-L). N=number of mice.

Q-X, Table 1). These mice either walk or gallop at lower speeds, and gradually change to all galloping gait as speed increases, with no appearance of discernable trotting. This result is comparable to the previous study of fictive locomotion in DCC KO neonatal mice, in which both L2 and L5 nerve roots display uncoordinated firing with the opposite side (Bernhardt et al., 2012). Since both DCC deficient groups are DCC deficient below cervical level, it is reasonable to conclude that their synchronized hindlimb movement is caused by the lack of DCC expression at lower spinal levels, possibly due to the defects of commissure neuron path finding thus the abnormal CPG formation. Interestingly, the synchronization of hindlimb movement is more severe in $mDCC^{f/-}$ compared to $mDCC^{f/f}$ (Figure 6P,T, Figure 7Q-T, U-X, Table 1), which is likely to be caused by certain descending tract defects in $mDCC^{f/-}$ due to the universal lower DCC expression. Both $mDCC^{f/f}$ and $mDCC^{f/-}$ mice do display some alternating hindlimb movement at the lower speed 15cm/s (Figure 7Q, U). It is also observed that both DCC deficient groups show a large percentage of out of phase forelimb coupling at all tested speeds (Figure 6N,R, Figure 7E-H, I-L), with $mDCC^{f/-}$ showing slightly more synchronized forelimb movement, which also result in their diagonal coupling value to shift toward 0.5 compared to control and heterozygous groups.

3.1.2 DCC Deficient Mice Reach Lower Maximum Speed

One thing we noticed while running the mice on the treadmill is that DCC deficient mice run considerably slower than the control animals. To test this hypothesis, we examined the maximum locomotion speed of each mouse in two ways. When given the same setting as the set speed treadmill locomotion trials, two $mDCC^{f/f}$ mice reach the maximum set speed of 35cm/s and the rest three in the group reach 45cm/s. In contrast, three out of

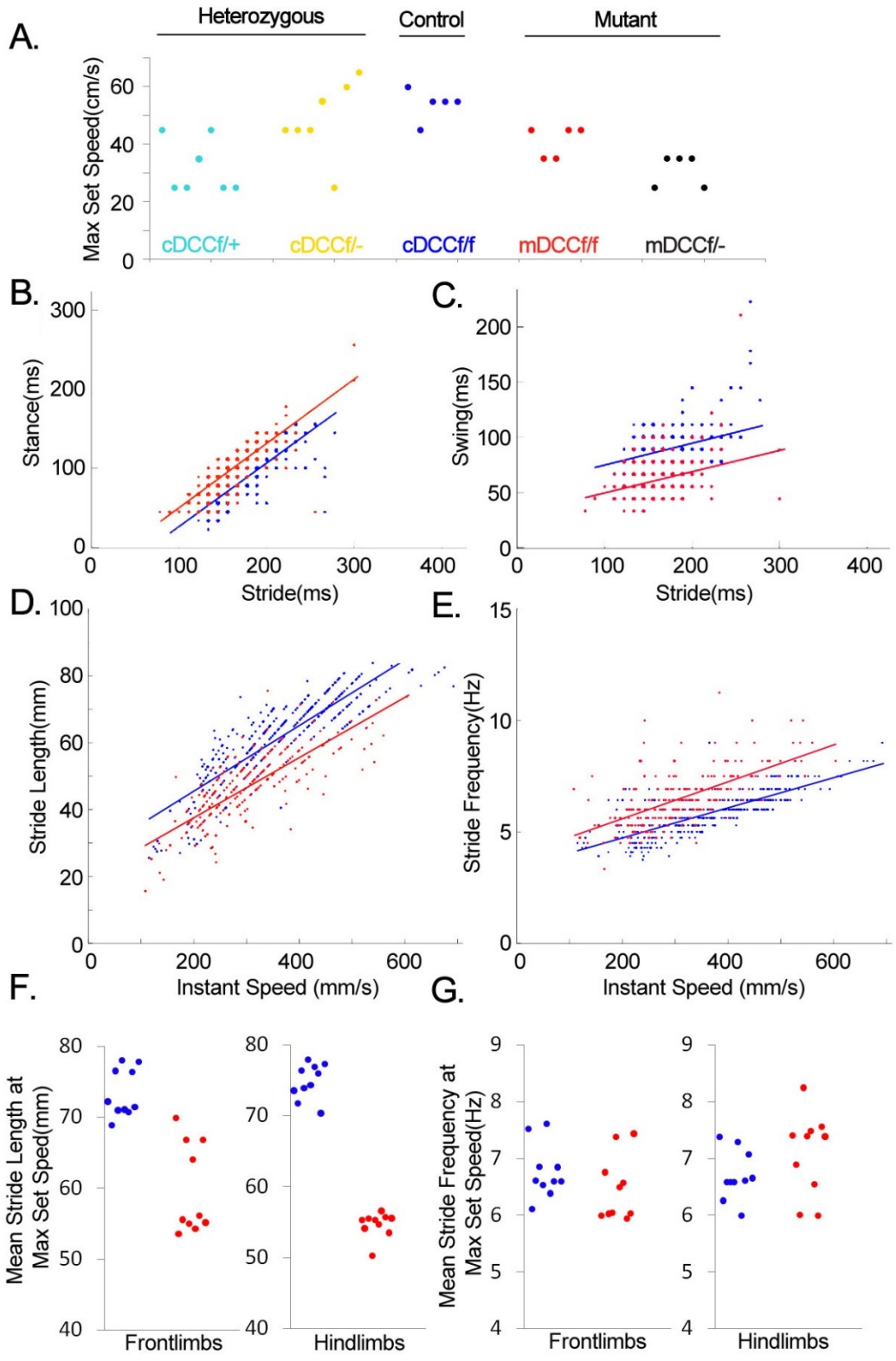
A.
Heterozygous
Control
Mutant
Max Set Speed(cm/s)
0
20
40
60
cDCCf/+
cDCCf/-
cDCCf/f
mDCCf/f
mDCCf/-
B.
Stance(ms)
0
100
200
300
0
100
200
300
400
Stride(ms)
C.
Swing(ms)
0
50
100
150
200
0
100
200
300
400
Stride(ms)
D.
Stride Length(mm)
0
20
40
60
80
100
0
200
400
600
Instant Speed (mm/s)
E.
Stride Frequency(Hz)
0
5
10
15
0
200
400
600
Instant Speed (mm/s)
F.
Mean Stride Length at Max Set Sped(mm)
40
50
60
70
80
Frontlimbs
Hindlimbs
G.
Mean Stride Frequency at Max Set Speed(Hz)
4
5
6
7
8
9
Frontlimbs
Hindlimbs

Figure 8. Maximum speed and step cycle analysis of DCC deficient and control mice. DCC deficient mice can reach lower maximum set speed on the treadmill compared to the controls (A, 1 data point = 1 mouse). DCC deficient mice have longer stance duration and shorter swing duration under all speeds (B,C). DCC deficient mice have shorter stride length and higher stride frequency at all speeds (D,E). The mean stride length at each mouse's maximum set speed is shorter in DCC deficient mice than controls for both forelimbs and hindlimbs (F, 1 data point = 1 limb, two limbs per mouse are used in each data set), but stride frequencies of both are similar between DCC deficient mice and controls (G, 1 data point = 1 limb, two limbs per mouse are used in each data set). In B-G, blue = data from cDCCf/f mice; red = data from mDCCf/f mice. In B-E, twenty steps per speed are used for each mouse, and five mice are used in each group. Data points appear overlapping as a result of the limitation by frame rate of the videos analyzed in Treadscan. In F-G, each data point is the mean value of at least twenty steps of the limb from the trial(s) representing the maximum set speed of the respective mouse. Data from both left side and right side limbs of the mouse are used in the graghs, each contributing to one data point. In B-G, red=mDCCf/f, blue=cDCCf/f.

five $cDCC^{f/f}$ mice can reach 55cm/s, 1 reaches 65cm/s, and only 1 has a maximum set speed of 45cm/s (Figure 8A). Similar results can be achieved using continuous speed increase method on more spacious treadmill to test the maximum speed, during which mice in both $mDCC^{f/f}$ and $cDCC^{f/f}$ group run faster than in the previous method, but $mDCC^{f/f}$ mice are still slightly slower than $cDCC^{f/f}$ mice (Data not shown).

Mice in $mDCC^{f/-}$ group are a little slower than $mDCC^{f/f}$, and mice in the two DCC heterozygous groups show a big variation in their maximum set speeds, ranging from 25cm/s to 65cm/s (Figure 8A). Since there could be a descending tract defect in $mDCC^{f/-}$ and $cDCC^{f/-}$ and a dosage effect in $mDCC^{f/-}$ and both the heterozygous groups, the rest of the study will be focused on the wildtype control $cDCC^{f/f}$ group, and $mDCC^{f/f}$ group, in which both DCC allelles are knocked out below cervical spinal cord.

In order to examine the reason of DCC deficient mice's slower speed, we examined several parameters of their step cycle, including stance duration, swing duration, stride length and stride frequency. Since the forelimb movement in the DCC deficient mice shows a big variation in the coupling study, we mainly focused on their hindlimb movements.

3.1.3 DCC Deficient Mice Show Longer Hindlimb Stance Duration and Shorter Swing Duration

At all locomotion speeds, DCC deficient $mDCC^{f/f}$ mice consistently show a longer stance and shorter swing duration compared to the control $cDCC^{f/f}$ mice (Figure 8B, C). Such result is in agreement with the prediction, since $mDCC^{f/f}$ mice have synchronized

hindlimb movements at all speeds as opposed to the alternating hindlimb movements in cDCC$^{f/f}$ mice, and synchronized hindlimb movements result in periods in the step cycle when both feet are in the air. Longer stance duration is therefore expected as an adaptation in need to support the body weight.

3.1.4 DCC Deficient Mice Have Shorter Hindlimb Stride Length and Higher Stride Frequency

At all locomotion speeds, the hindlimbs of mDCC$^{f/f}$ mice also consistently show a shorter stride length and a higher stride frequency than that of cDCC$^{f/f}$ mice (Figure 8D, E). Since the locomotion speed is dependent on both stride length and stride frequency, we hypothesized that the slower locomotion speeds in mDCC$^{f/f}$ mice is caused by their limited stride length. Interestingly, when we analyzed the mean stride length and frequency at each mouse's maximum set speed, it shows that the stride length of mDCC$^{f/f}$ is much shorter than that of the cDCC$^{f/f}$, while the stride frequency of the mDCC$^{f/f}$ is only slightly higher (Figure 8F, G). This is true for both forelimbs and hindlimbs, while hindlimb stride lengths show much smaller variation amongst individuals in the same group, indicating itself being the primary cause of mDCC$^{f/f}$'s slower locomotion speed. The slightly higher stride frequency of mDCC$^{f/f}$ mice could be a partial compensation of the shorter stride length in order to keep up with the locomotion speed.

From the above results, it can be concluded here that shorter hindlimb stride length is the limitation of locomotion speed in DCC deficient mice, which is partially compensated by higher stride frequency.

3.2 NCK2 Knockout Mice

3.2.1 Nck2 KO Mice Display More Out of Phase Interlimb Coupling and More Abnormal Step Sequence

In the study of the effect of Nck2 on locomotion, we first tested the Nck2 knockout ($Nck2^{-/-}$) and heterozygous ($Nck2^{+/-}$) mice on treadmill under the same set speeds as in the DCC study, and compared their interlimb coupling with that of the control animals ($cDCC^{f/f}$).

Under all tested speeds, Nck2 KO mice show more dispersed distribution of both forelimbs homologous and hindlimbs homologous coupling as well as diagonal coupling, with the mean values of both homologous couplings shifting further away from 0.5 compared to control animals (Figure 9A-R, Table 1). It is noteworthy that such difference in interlimb coupling is not caused by different stride frequencies of the paired limbs (one leg is not moving faster than the other), but instead by the more frequent appearance of the occasional abnormal step sequence in continuous locomotion. $Nck2^{-/-}$ mice show a higher percentage of abnormal step sequence at all tested speeds (Figure 9S), which suggests a problem with interlimb coordination. The appearance of abnormal step sequence in $Nck2^{-/-}$ mice is even more frequent at lower speeds like 8cm/s and 15cm/s compared to middle and higher speeds from 25cm/s to 45cm/s. The dramatic drop of normal step sequence percentage of $Nck2^{-/-}$ mice a t 55cm/s is caused by their struggle to catch up with the speed, which results in a lot of sudden jumping as a way of acceleration in this situation.

The interlimb coupling results of the heterozygous $Nck2^{+/-}$ animals are not different from controls at 25cm/s. However, since two of the six available $Nck2^{+/-}$ mice are unwilling to run on the treadmill, and three of the four that are willing cannot reach speed higher than 35cm/s, it is statistically insufficient to describe their interlimb coupling at higher speeds.

The incapabilily of the $Nck2^{+/-}$ mice to run at higher speed is not necessarily caused by changes in spinal locomotor network. Some of the $Nck2^{+/-}$ mice are able to run faster when given more space and some acoustic stimulation on the treadmill, but cannot reach the same speed under our standard treadmill trial circumstances even with additional training. Moreover, many $Nck2^{+/-}$ mice display freezing behavior after trials, which took as long as 20 minutes to recover, indicating the severity of the fear the mice experience. The above symptoms are understandable since the systemic reduction of Nck2 expression may affect brain and descending pathways, which may be the cause of the $Nck2^{+/-}$ mice's incapability to run at higher speeds. In fact, four of the eleven $Nck2^{-/-}$ animal displayed similar symptoms and were not usable in the study.

During the interlimb coupling analysis, it is noticeable that some $Nck2^{-/-}$ mice often have an additional lift of foot toward the end of swing phase before the foot contacts the ground. In some cases, the additional foot lift happens after the foot contacting ground, which results in an additional step of that foot in the analysis, thus the appearance if an abnormal step sequence. In order to investigate this phenomenon, we studied the step cycle and joint angle change in these animals in the following study.

3.2.2 Nck2 KO Mice Show a Phase Shift in Joint Angle Changes

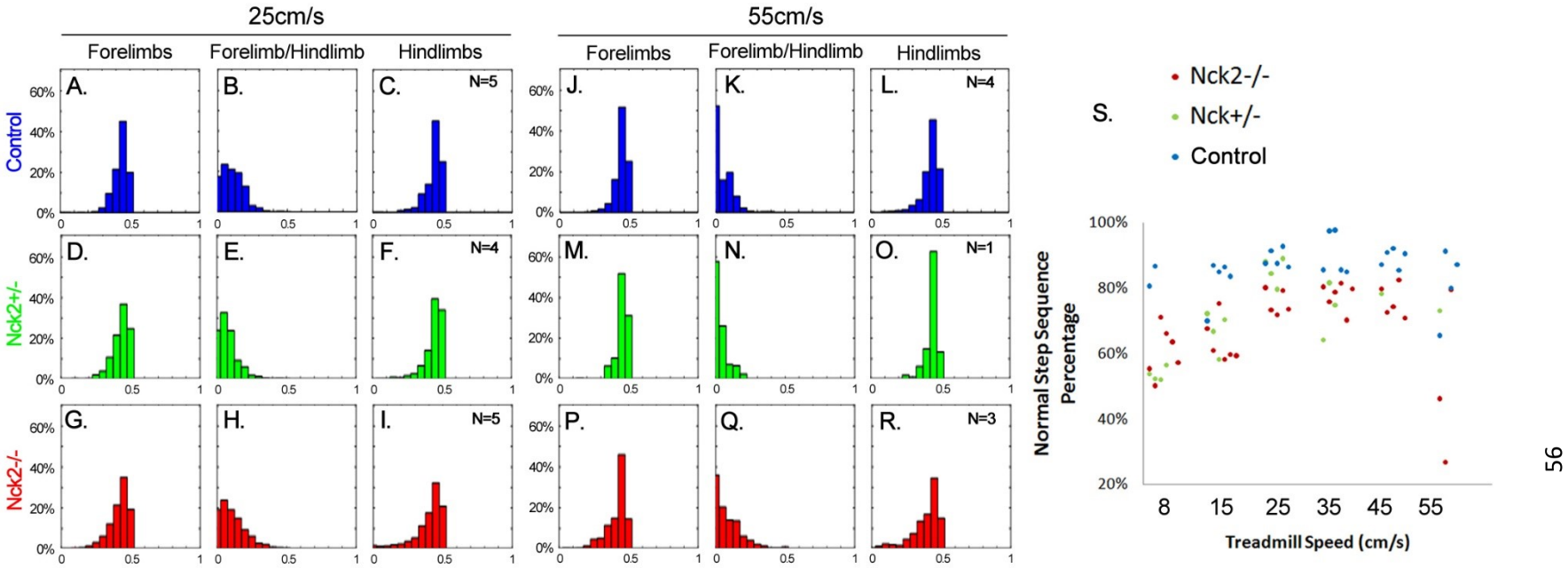

Figure 9. Nck2 KOs show more out of phase interlimb coupling as a result of higher frequency of abnormal step sequence.

Nck2 KO mice show more dispersed interlimb coupling value at both low and high speeds, while heterozygous mice display a coupling phenotype in between controls and KOs(A-R, N=number of mice). Nck2 KO mice show lower percentage of normal step sequence at all tested speeds (S, 1 data point = 1 mouse).

In the following study, due to the limited availability of testable animals, we use $Nck2^{-/-}$ mice as Nck2 KOs and $Nck1^{+/-}$;$Nck2^{f/f}$ mice as controls.

When we analyze the joint angle change in reference to the step cycle(the entire stride), the shapes of the hip, knee and ankle joint curve do not differ in the $Nck2^{-/-}$ and control animals. However, there is an apparent delay of joint angle change in the $Nck2^{-/-}$ mice compared to that of the controls (Figure 10B, left panel). Interestingly, when we analyze the joint angle change in reference to stance duration and swing duration separately, no such delay is observed (Data not shown). Similar results are achieved if hip and knee joint angle change is analyzed in reference to the four ankle phases separately, in which $Nck2^{-/-}$ do not delay from controls (Figure 10B, right panel).

We can also notice that the ankle angle around ankle p1, which is the time around the start of stance, is slightly larger in Nck2 KOs than controls (Figure 10B, right panel, third row). At the same time, a difference in paw angle around and after ankle p1 can be observed between the two groups (Figure 10B, right panel, bottom row). Control animals have an increase of paw angle at ankle p1, while Nck2 KO mice display a smooth decrease of the paw angle across ankle p1. Such difference is caused by the slight difference of the way two groups of mice contact the ground. More specifically, at the end of swing phase, our control animals contact the ground with their paws leading followed by the toes, which results in a plateau or even slight increase in paw angle around the time of contact. In contrast, the Nck2 KO mice contact the ground toe first followed by paw, which results in a smooth and continuously decreasing paw angle curve

around the contact. The difference in the paw angle also results in the slightly larger ankle angle in Nck2 KOs around this period.

The above results strongly suggest that there is an increase of swing phase in proportion to the step cycle in Nck2$^{-/-}$ animals. It can also be indicated that the proportion of the four ankle phases in Nck2$^{-/-}$ animals may be different from those in controls. Thus, we investigated these questions in more details in the following study.

3.2.3 Nck2 KO Mice Have Elongated Swing and Shortened Stance Duration

When we analyze the step cycle of the Nck2 KO and control animals by dividing it into stance and swing, we discovered that stance duration in Nck2 KO mice is shorter than that of the controls and swing duration longer (Figure 10C). This is true under all tested speeds. This explains the phase shift in the joint angle curves described in the previous section. Interestingly, the difference in stance and swing duration is bigger at lower running speed, or when stride duration is longer (Figure 10C), which means Nck2 KO animals have more severe problems at lower speeds. It also indicates that the swing duration in the Nck2 animas is more dependent on stride duration (swing/stride slope= 0.2635, R^2=0.5044) compared to the control animals (swing/stride slope= 0.1159, R^2=0.4477), and consequently, their stance duration less dependent on stride duration (stance/stride slope= 0.7365, R^2=0.8883) than the controls (stance/stride slope= 0.8841, R^2=0.9792).

3.2.4 Hip and Ankle Cycle Change in Nck2 KO Mice

Next we analyzed the flexor and extensor phases of the hip and ankle joints of Nck2 KO and control mice.

In $Nck2^{-/-}$ mice, the hip flexor phase is longer than that in the controls under all speeds (Figure 10D, top panel), and correspondently, the hip extensor phase is shorter (Figure 10D, bottom panel). When we look at the four ankle phases, in $Nck2^{-/-}$ mice, both the ankle flexor phase and E1 phase are longer than those of the controls (Figure 10E, top two panels), and E3 phase is shorter (Figure 10E, bottom panel). Ankle E2 phase, on the other hand, does not differ in the Nck2 KO and control animals (Figure 10E, third panel). The added effect of longer ankle F and E1 phase in Nck2 KOs is the corresponding longer swing phase in a step cycle, as described above.

It is intriguing that hip phase difference is considerably consistent at all speeds (control: Hip F/Hip cycle slope= 0.2304, R^2=0.5096; Nck KO: Hip F/Hip cycle slope= 0.3165, R^2=0.5024), while the differences in ankle phase cycle is bigger at lower speeds, but decreases dramatically as the speed increases (control: Ankle F/Ankle cycle slope= 0.0713, R^2=0.27; Ankle E1/Ankle cycle slope=0.0503, R^2=0.2118; Ankle E3/Ankle cycle slope= 0.6336, R^2=0.8674; Nck2 KO: Ankle F/Ankle cycle slope= 0.1395, R^2=0.2905; Ankle E1/Ankle cycle slope= 0.1339, R^2=0.2879; Ankle E3/Ankle cycle slope= 0.4805, R^2=0.741). This indicates that Nck2-/- mice have more severe problem at proximal part of the limb than the distal parts.

3.2.5 EMG Changes in Nck2 KO Mice

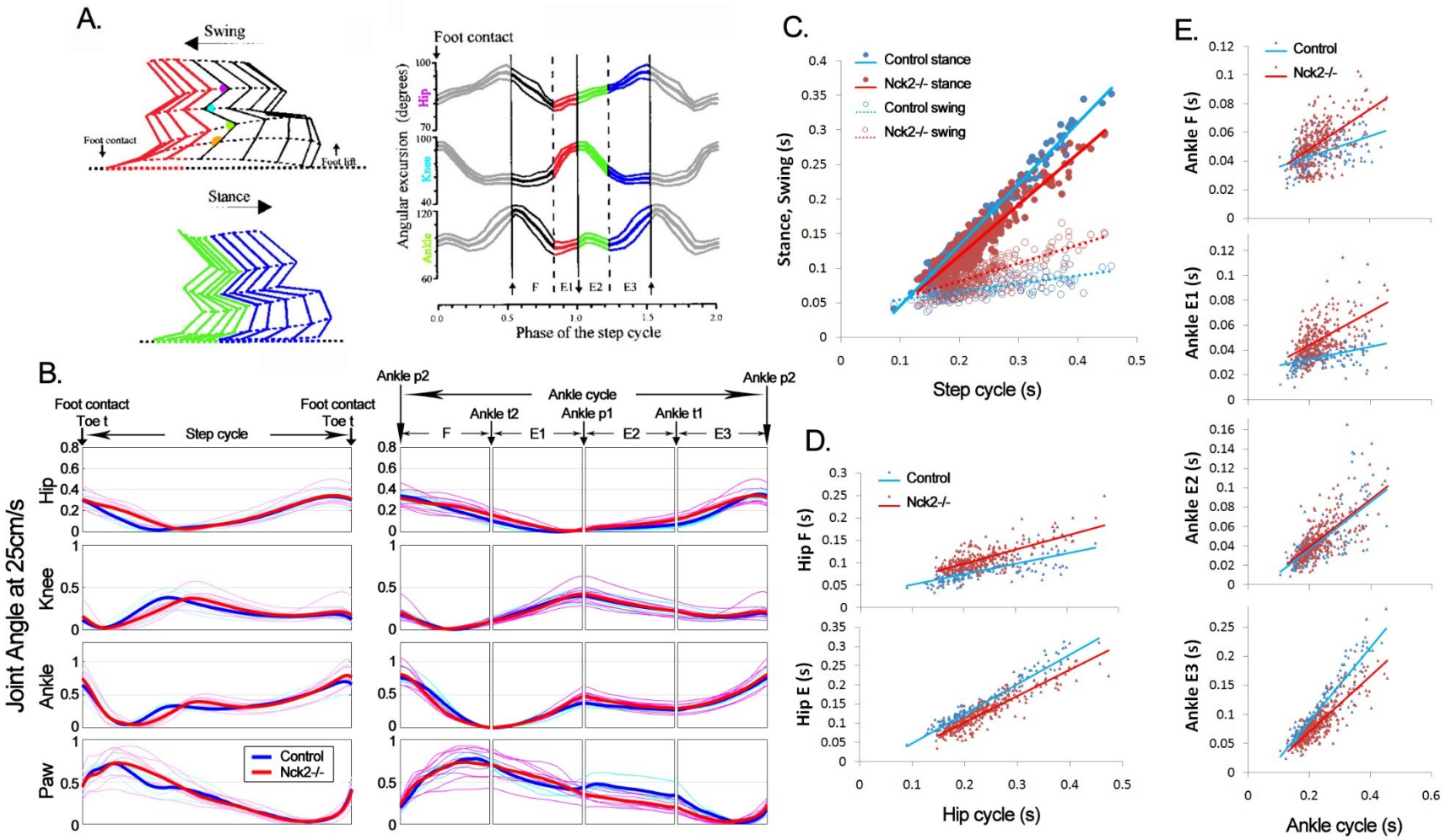
A.
Swing
Foot contact
Foot lift
Stance
Foot contact
Angular excursion (degrees)
Hip
Knee
Ankle
F
E1
E2
E3
Phase of the step cycle
B.
Foot contact
Toe t
Step cycle
Foot contact
Toe t
Ankle p2
Ankle cycle
Ankle p2
Ankle t2
Ankle p1
Ankle t1
F
E1
E2
E3
Joint Angle at 25cm/s
Hip
Knee
Ankle
Paw
Control
Nck2-/-
C.
Control stance
Nck2-/- stance
Control swing
Nck2-/- swing
Stance, Swing (s)
Step cycle (s)
D.
Control
Nck2-/-
Hip F (s)
Hip E (s)
Hip cycle (s)
E.
Control
Nck2-/-
Ankle F (s)
Ankle E1 (s)
Ankle E2 (s)
Ankle E3 (s)
Ankle cycle (s)

Figure 10. Joint angle change and step and joint cycle analysis of Nck2 KO and control mice.

Illustration of step cycle and ankle joint cycle phase (A). Joint angle change at 25cm/s in Nck2 KO step cycle shows a phase change compared to the control (B left), which corresponds to Ankle joint phase as the two groups don't show hip and knee angle difference when analyzed using ankle joint phase as reference (B right). Six hindlimbs from three control mice (Nck1+/-;Nck2f/f) and nine hindlimbs from five Nck2 KO mice (Nck2-/-) are used in joint angle curves generation. Each curve in (B) is the mean of at least twenty steps. Each thin curve represents the mean of one limb. Thick curve represents the mean of all limbs. Nck2 KOs have shorter stance and longer swing phase compared to controls, which is more dramatic at lower speed (C). Nck2 KOs have longer hip flexor phase (Hip F) and shorter hip extensor phase (Hip E) at all speeds (D). Nck2 KOs also have longer ankle flexor (F) and extensor I (E1) phases but shorter ankle extensor III (E3) phase, which are more dramatic at lower speeds, but the length of ankle extensor II (E2) phase is not different from controls(E). In (C,D,E), sixty steps per mouse from three control and two Nck2 KO animals are used in each sub-figure.

In order to further investigate the nature of step cycle, hip cycle and ankle cycle changes in Nck2 KO animals, we recorded and analyzed the EMG signals from the hip flexor (IP), hip extensor (BF), ankle flexor (TA) and ankle extensor (GS) muscles from the two groups of mice during fixed speed treadmill locomotion (muscle location illustrated in Figure 11A).

Similar to joint angle curves, EMG curves generated in reference to the whole step cycle show a phase shift between Nck2 KOs and controls (Figure 11D, left panel). Under the speed of 15 and 25cm/s, the activation time of IP and TA in $Nck2^{-/-}$ mice are both longer than those in controls (Figure 11D, left panel). However, if EMG signal is normalized in reference to the ankle cycle, the activation of the two muscles cover the same ankle phases in both groups, e.g. IP activation starts at late E3 and ends at the end of E1, covering almost the whole swing phase in a step cycle, and TA activation starts at late E3 and ends at the end of ankle flexor phase (Figure 11C, D right panel). Similarly, BF and GS muscle in both groups also have the same coverage in ankle cycle (Figure 11B, C, D right panel). In summary, in $Nck2^{-/-}$ mice, all the four muscles tested do not alter their activation time in reference to the ankle cycle. As a result, no additional overlapping between paired flexor and extensor is observed in $Nck2^{-/-}$ animals, which suggests that they are not likely to have problems in ipsilateral flexor/extensor alternation, a function controlled by V1 and V2b interneurons (Zhang et al., 2014).

It is also observed that the shape of the BF and GS EMG curves is different in Nck2 KOs and controls (Figure 11D, second and fourth row). In control mice, BF activation starts at mid E1 phase, and gradually increases its amplitude which peaks shortly after the

beginning of E2 phase. In Nck2$^{-/-}$ mice however, BF amplitude has a sudden increase shortly after its activation (Figure 11D, right panel second row, yellow arrowhead), creating an additional plateau or peak during E1 phase in the curve. GS activation in control mice remains minimum throughout E2 and starts to increase in amplitude at the beginning of E3 phase, and peaks around mid E3. In contrast, GS activation in Nck2$^{-/-}$ mice sometimes reaches much bigger amplitude as soon as it is activated in mid E1 and maintains that amplitude throughout E2 phase (Figure 11D, right panel bottom row, yellow arrowhead). The bigger amplitude of BF and GS muscle EMG signals early in their activation in Nck2$^{-/-}$ mice could serve as a compensation for the animal's elongated swing duration, as it is needed for the added weight support during the longer swing of the contralateral limb.

It should be noticed that the steeper increase of BF and GS signal in their beginning part in Nck2$^{-/-}$ mice as shown in ankle phase normalized EMG curves is not obvious if EMG signals are normalized according to the whole step cycle, as shown in Figure 11D left panel. This is because each Nck2$^{-/-}$ mouse shows a bigger variance in the lengths of its step and ankle cycle phases (indicated in Figure 10C, E and Figure 11B, C). As a result, the steeper increase of EMG signals in mid E1 phase of each step are neutralized and not observed if the EMG curve is not normalized to ankle phase. By normalizing the EMG signals to ankle phases, we were able to expose this relative subtle phenotype of the Nck2$^{-/-}$ mice which is harder to observe otherwise. It should be noticed as well that the EMG signals also show relative bigger variance amongst Nck2$^{-/-}$ individuals, which reflect the variation between these animals in the severity of their phenotypes. A bigger sample size would be helpful to depict the phenotype of this group more accurately.

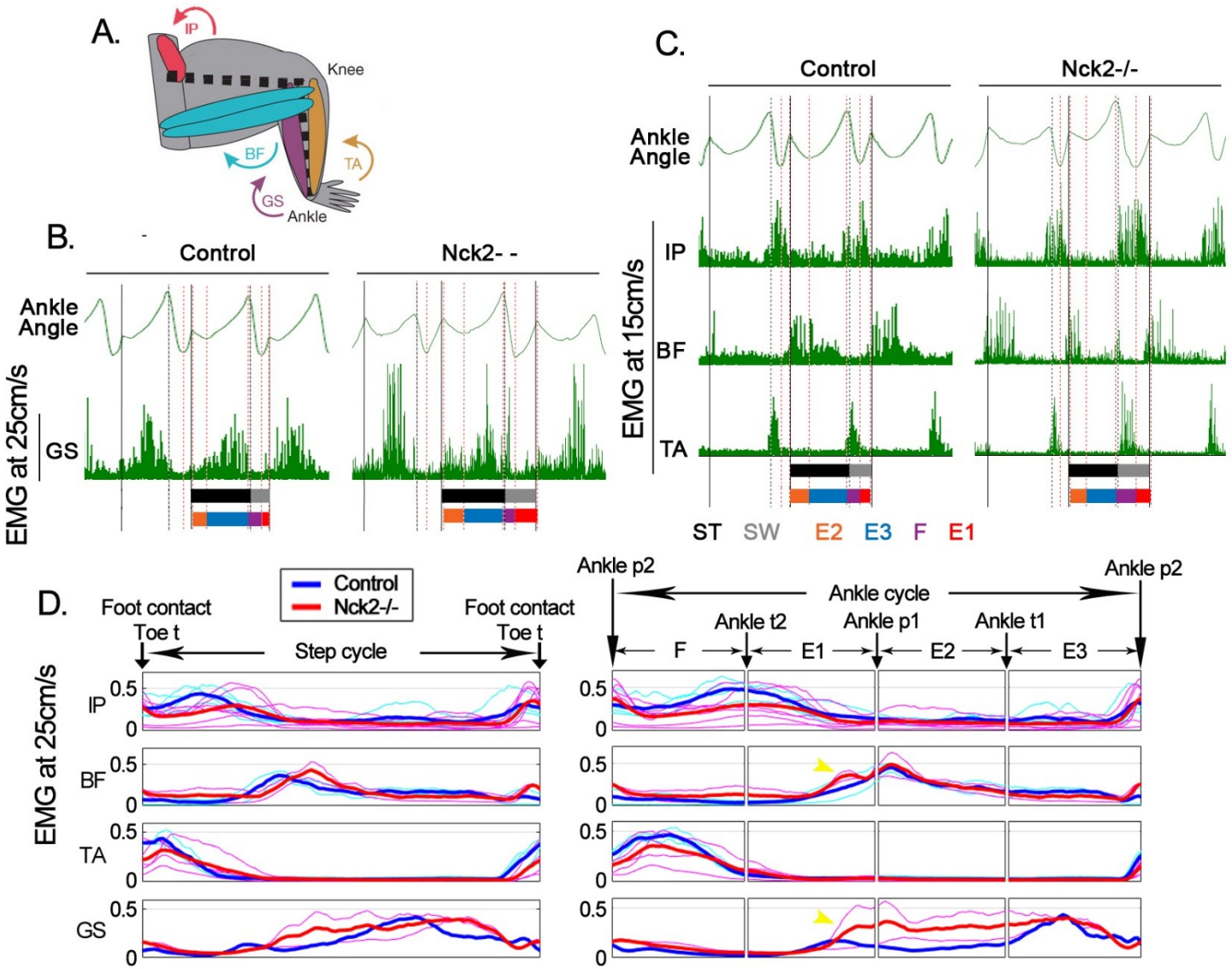
A.
IP
Knee
BF
TA
GS
Ankle
B.
Control
Nck2- -
Ankle Angle
EMG at 25cm/s
GS
C.
Control
Nck2-/-
Ankle Angle
EMG at 15cm/s
IP
BF
TA
ST SW E2 E3 F E1
D.
Control
Nck2-/-
Foot contact
Toe t
Step cycle
Foot contact
Toe t
Ankle p2
Ankle cycle
Ankle p2
Ankle t2
Ankle p1
Ankle t1
F E1 E2 E3
EMG at 25cm/s
IP
BF
TA
GS
0.5
0

Figure 11. EMG analysis of Nck2 KO and control mice.

Illustration of muscles of EMG implantation (A). IP= Iliopsoas (hip flexor), BF=Bicep femoris (hip extensor and knee flexor), TA=Tibialis anterior (ankle flexor), GS=Gastrocuemius-soleus (ankle extensor). EMG examples at 15cm/s (C) and 25cm/s (B) and collective curves at 25 cm/s (D) all show that Nck2 KOs have longer IP and TA activation, but both are in phase with ankle angle phases. BF and GS in Nck2 KOs have stronger activation at the beginning of stance. In (D), four hindlimbs from three control mice (Nck1+/-;Nck2f/f) and seven hindlimbs from 5 Nck2 KO mice (Nck2-/-) are used in IP curves generation; two limbs from one controls and two limbs from two Nck2 KOs are used for BF curves; three limbs from two controls and five limbs from four Nck2 KOs are used for TA curves; one limb from one control and two limb from two Nck2 KOs are used for GS curves. Each curve in (D) is the mean of at least twenty steps. Each thin curve represents the mean of one limb. Thick curve represents the mean of all limbs.

	Coupling Mean±Standard Deviation (Number of Mice)				
	Forelimbs				
Treadmill Speed (cm/s)	15	25	35	45	55
$mDCC^{f/-}$	0.3047±0.151(7)	0.2252±0.1381(7)	0.2298±0.1268(4)	0.2272±0.084(1)	
$mDCC^{f/f}$	0.317±0.1453(5)	0.3245±0.1212(5)	0.3162±0.1212(5)	0.3799±0.0889(3)	
$cDCC^{f/+}$	0.4109±0.0728(7)	0.4262±0.0583(7)	0.4259±0.0333(2)	0.4611±0.0372(2)	
$cDCC^{f/-}$	0.4042±0.0768(7)	0.42560.0644(7)	0.4442±0.0498(6)	0.4499±0.0482(6)	
$cDCC^{f/f}$(Nck2 Control)	0.4169±0.0708(5)	0.4331±0.0597(5)	0.4438±0.0495(5)	0.4538±0.0427(5)	0.4487±0.0489(4)
$Nck2^{+/-}$		0.4297±0.0582(4)	0.4326±0.0585(3)	0.4476±0.0451(1)	0.4552±0.0455(1)
$Nck2^{-/-}$		0.4125±0.0761(5)	0.4246±0.0656(6)	0.4201±0.0756(5)	0.4137±0.0814(3)
	Hindlimbs				
Treadmill Speed (cm/s)	15	25	35	45	55
$mDCC^{f/-}$	0.1511±0.1719(7)	0.071±0.0895(7)	0.0723±0.0672(4)	0.0439±0.0594(1)	
$mDCC^{f/f}$	0.1783±0.1743(5)	0.148±0.1346(5)	0.1285±0.1064(5)	0.1147±0.1173(3)	
$cDCC^{f/+}$	0.4007±0.0937(7)	0.4378±0.0586(7)	0.4542±0.0035(2)	0.4537±0.0419(2)	
$cDCC^{f/-}$	0.3995±0.0959(7)	0.4321±0.0723(7)	0.4515±0.0549(6)	0.4534±0.0497(6)	
$cDCC^{f/f}$(Nck2 Control)	0.3986±0.0931(5)	0.4341±0.0717(5)	0.4522±0.0461(5)	0.4491±0.0498(5)	0.4313±0.0696(4)
$Nck2^{+/-}$		0.4396±0.0648(4)	0.4391±0.0654(3)	0.4386±0.0551(1)	0.4391±0.0471(1)
$Nck2^{-/-}$		0.3941±0.1095(5)	0.418±0.0838(6)	0.4119±0.0851(5)	0.3874±0.1052(3)

Table 1. Homologous Coupling Mean Value and Standard Deviation

Forelimbs homologous coupling and hindlimb homologous coupling mean value for each group are shown. Standard deviations here indicate variation between individuals. Number of mice in each group is also indicated. Mean±Standard Deviation(Number of mice).

CHAPTER 4 DISCUSSION

4.1 Summary of Findings

In the study of DCC deficient mice, we described the treadmill locomotion in adult animals. DCC deficiency in the spinal cord results in synchronized hindlimb movement in the DCC deficient mice under all speed, which is even more uniform under higher speed. It also results in a difference in locomotion speed, that DCC deficient mice can reach lower maximum speed than the wildtype control mice. The speed in the DCC deficient mice is limited by their shorter stride lengths, and partially compensated by their higher stride frequency. The hindlimb stance duration in DCC deficient mice is longer than that in the controls and swing duration shorter as a result of their hopping gait.

In the study of Nck2 KO mice, we discovered that Nck2 single knockout results in increased out of phase interlimb coupling and the appearance of more abnormal step sequence. The hindlimb swing duration is increased in the $Nck2^{-/-}$ animals, and the stance duration is decreased. Joint angle changes in the $Nck2^{-/-}$ animals show a phase shift in alliance with the increased swing phase. Nck2 KO also caused elongated ankle flexor and extensor 1 phases, as well as shortened ankle extensor phase 3 as compensation. $Nck2^{-/-}$ animals also have longer firing length in hip and ankle flexor muscles paralleled to their altered step cycle and joint angle phases, and stronger and more abrupt activation of hip and ankle extensor muscles in the middle of ankle E1 phase where their activation begins, possibly as a weight support method in compensation for the elongated swing phase in the opposite limb.

4.2 The Genetics of DCC Deficient Mice Strains and the Implication

In our study of DCC's function in locomotion, five strains of mice are used. It is important to understand the genetics of the five strains, thus understanding the opportunity this method provides as well as the limitations it brings.

The generation of these mice utilized both straight knockout of DCC and conditional DCC knockout induced by Hoxb8 expression. Such genetic manipulations create the following differences in the resulted mice strains: 1) the spatial expression of DCC; 2) the onset of DCC deficiency; 3) the completeness of DCC deficiency.

In both $mDCC^{f/-}$ and $cDCC^{f/-}$ groups, one allele of DCC is knocked out independently from Hox8b expression, which means in these two strains DCC expression level is expected to be reduced at higher levels of the CNS, including brains and descending tracts. The reduction of DCC may affect brain development, since DCC is widely expressed in all developing neuronal tissues and regulate neuronal pathfinding in brains as well. Indeed, DCC deletion from adult forebrain neurons results in impaired spatial memory and recognition in mice, which is probably caused by loss of long term potentiation (LTP) and shorter dentritic spines (Horn et al., 2013). This may explain the lower locomotion speed in $mDCC^{f/-}$ group compaired to $mDCC^{f/f}$, that although DCC depletion in lower spinal cord cause gait change in both groups, reduction of DCC expression at higher levels in the $mDCC^{f/-}$ mice cause their unwillingness to run faster, or else their incapability to learn to catch up with the increased treadmill speed.

The Hoxb8 dependent DCC knockout limits DCC reduction both spatially and temporally. Spatially, Hoxb8 as a homeobox gene and theoretically has a sharp rostral expression border at C2 (Charité et al., 1995). Witschi and colleagues. described the spatial distribution of cre-mediated gene recombination in the Hoxb8-cre mice by examining LacZ expression in Hoxb8-Cre^{tg+}/R26R mice. LacZ was expressed at high level in all neurons and glials at thoracic and lumbar segments, but expression started to disappear around C4 and was only expressed in a few scattered cells in the grey matter at C2 (Witschi et al., 2010). The group explains this difference with the lack of a retinoic acid-responsive element between Hoxb4 and Hoxb5 in the Hoxb8-cre construct (Oosterveen, 2003; Valarche et al., 1997). Fortunately, no expression of LacZ is detected in the brain (Witschi et al., 2010). In our study, TdTomato expression in the mDCC$^{f/f}$ strain indicated that cre activation has a gradual change at its rostral border. More specifically, Tomato expression in the spinal cord decreases caudal-rostrally from T1 forward, and is almost completely invisible around C3/4. This is a more caudal expression pattern than described before. Moreover, the rostral borders of Tomato expression in each mDCC$^{f/f}$ mice show a subtle variance about two segments long. Since forelimb CPG is located around C8-C9 level, the mixed forelimbs coupling pattern could be a result of different DCC deletion situation in each mice. mDCC$^{f/-}$ generally show more synchronized movement in the forelimbs than mDCC$^{f/f}$ because of a lower expression of DCC at cervical spinal cord due to the straight knockout of one of its DCC alleles. Therefore, our results indicate that cervical locomotor CPG formation may also involve DCC expression in a similar way to lumbar locomotor CPG.

Temporally, indogeneous Hoxb8 expression initiates early in development at head fold stage (E7.5-E8.5, Charité et al., 1995), while the earliest detection of DCC mRNA is after E8.5 (Gad et al., 1997). This eliminates the possibility of temporal difference of DCC expression in the lumbar spinal cord, which would be a factor that causes the difference in $mDCC^{f/f}$ and $cDCC^{f/f}$ mice.

Finally, the efficiency of cre expression is always debated in all cre-induced genetic modulation systems. According to Witschi and colleagues, lacZ activation in the Hoxb8-Cre^{tg+}/R26R mice is detected in all neurons and glias in the lumbar spinal cord (Witschi et al., 2010), which lends strong evidence to the presumably high efficiency of cre-induced lumbar DCC deletion in our mice. Nevertheless, in situ detection of DCC mRNA or immunohistochemical detection of DCC protein in the embryos of these mice would provide stronger support.

4.3 Nck2's Relationship with DCC in Locomotion

According to the results of this study, the locomotion phenotypes in DCC deficient and Nck2 KO adult animals are very different. DCC mutation in the spinal cord majorly cause the loss of left-right alternation in the hindlimbs, while Nck2 KO causes alteration in step and joint cycle formation without noticeable change in left-right alternation. Such difference in phenotype on top of the different expression pattern of DCC and Nck2 in the spinal cord (Gad et al., 1997; Lane, Qi and Fawcett, 2015) strongly suggest their different functions in locomotion. Nck2 elicits its function in locomotion at least partly through a DCC independent pathway, possibly through its interaction with EphA4, Ephrin B3 or Robo, as all are involved in spinal interneuron circuit development.

It should be noted that we are not excluding the possibility that part of Nck2's function here is via its interaction with DCC. Indeed, Nck2 and DCC are co-expressed at the ventral midline of the spinal cord (Lane, Qi and Fawcett, 2015). Although in vitro studies have indicated that only Nck1 constitutively binds to DCC, it cannot be ruled out that Nck2 is functionally redundant to Nck1 in the sense of commissure formation involving DCC.

It is worth noticing that our study in the DCC deficient animals show that loss of DCC in the spinal cord result in synchronized hindlimb movement, as opposed to the more severe complete left-right uncoordination observed in the fictive locomotion of neonatal DCC KO animals (Bernhardt et al., 2012). Such difference is possibly caused by two reasons. Firstly, systemic loss of DCC may affect higher levels of locomotion control like CST, since DCC is ubiquitously expressed in all neuronal tissues during development. In contrast, DCC mutation in our animals only causes the complete deletion below C2. Secondly, such phenotypic difference might indicate that adult DCC deficient animal have some level of adaptation to the uncoordinated gait in the newborns. To test these hypotheses, fictive locomotion tests should be performed in our DCC conditional knockout newborn mice and the result should be compared to those in the DCC KO animals. Anatomy studies should also be performed to investigate the remaining excitatory and inhibitory INs in the spinal cord of our DCC deficient mice used in this study.

4.4 Nck2 in Different Neuronal Groups

The expression of Nck2 in the midline region during early development strongly suggests its role in commissure formation. However, our results in the Nck2 KO animal show minimal alteration in left-right coordination. One possibility is that loss of Nck2 affect both excitatory and inhibitory commissure interneuron populations, possibly causes a reduction in both as indicated by the slightly thinner ventral commissure bundles (Lane, Qi and Fawcett, 2015). As a result, the proportion of commissural excitatory/inhibitory input is maintained, thus no loss of alternation is observed in the animals.

Since Nck2 expression is down-regulated in most spinal regions later in development, another possibility is that Nck2 depletion affect locomotion through the loss of its function in motor neurons instead of in the pre-motor network. The elongated flexor muscle activation and shortened extensor muscle activation in the Nck2 KO animal could be an indicator of altered flexor-extensor phase transition, which could result from reduced inhibitory feedback signals to the flexor MNs from either RCs or group I or group II afferents (Perreault et al. 1995; Hiebert et al. 1996; Stecina et al. 2005; Wang et al., 2008; Nishimaru and Kakizaki, 2009). It could be assumed that Nck2 depletion affect flexor MNs more severely than extensor MNs, and causes the flexor MNs to be less responsive to the inhibitory feedback signals. However, to test this hypothesis, electrophysiological properties from the MNs in the flexor and extensor pools need to be directly investigated in the Nck2 KO animal.

Although in situ hybridization study shows Nck2 has very low mRNA level in most other interneuron groups especially later in development, its potential function in these interneurons cannot be ruled out since protein expression level has not been directly

tested. It is also possible that Nck1 or Nck2 single knockout in the mice may result in the overexpression or ectopic expression of the other as a compensational effect. The exact cell type Nck2 affects in locomotor formation remains to be studied by conditionally knocking out Nck2 in these cell types.

4.5 Future Directions

4.5.1 Uphill and Downhill Treadmill Locomotion in Nck2 KO Mice

During uphill (climbing) or downhill treadmill locomotion, sensory feedback is increased comparing to locomotion on horizontal surfaces. In Nck2 KO animals, we observed an increase in the swing phase and a decrease in the stance phase. Such change in step cycle became less dramatic as the locomotion speed increases. One possible explanation for this phenomenon is that Nck2 depletion causes reduced reception of sensory feedback, and the phenotype became less obvious when sensory feedback input is increased at higher speed. In order to test this hypothesis, uphill and downhill locomotion trials should be performed on the Nck2 KO mice to study if the change in step cycle and joint ankle cycle can be reversed, and thus understanding the condition of sensory feedback in these animals.

4.5.2 Fictive Locomotion in DCC Deficient and Nck2 KO Mice

Drug induced fictive locomotion test should be performed on newborn DCC deficient mice and Nck2 KO mice to test if the phenotypes are comparable to treadmill locomotion. Dorsal root stimulation can also be applied in these studies to investigate the potential sensory feedback problems in these mice. In addition, the proportion of excitatory/inhibitory input to the locomotor circuits in these animals can be studied by

applying specific chemical blocker like sarcosine, and observing if the loss of asynchronization in DCC deficient mice and the alteration in step cycle phase in Nck2 KOs can be reversed.

4.5.3 Conditional Knockout of Nck2 in Different Interneurons

In order to understand Nck2's distinct function, we propose here to generate conditional Nck2 knockout animals targeting the mutation in Lhx3 (V2), En1 (V1), Sim1 (V3), and Dbx1 (V0) expressing populations respectively. Step cycles and joint angle cycles in these animals should be studied in treadmill locomotion and fictive locomotion, and compared to the results achieved in our study.

4.6 Limitations

Our study of the DCC deficient mice is greatly limited by the availability of mice. It would be interesting to do some anatomical study of the commissure formation by dye tracing in the embryonic stages, and check the DCC expression pattern in the five strains. It would also be interesting to look at the fictive locomotion in younger animals and compare it to locomotion in the adult animal. A comparison between neonatal locomotion in our DCC deficient mice and that in the $DCC^{-/-}$ mice, which has been formerly described as uncoordinated left-right coordination, would be helpful to understand the function of adaptation or sensory feedback in our DCC deficient mice. Furthermore, joint angle and EMG studies in the DCC deficient mice would be helpful to better understand intralimb coordination, if animals meeting the facility's standard of hygiene was available so that the performance of these experiments could be allowed.

In the study of Nck2 mice, to ensure proper control of genetic background, Nck2 heterozygous and homozygous control mice would be better controls to use for these studies. However, since many from these strains were unwilling to run, we compared the Nck2-/- mice, whose genetic background was mainly C57BL6 with mixed strain mice ($cDCC^{f/f}$). Although this is not ideal, the three strains used in Nck2 study do produce mice of similar weight and body type (no under or overweight mice in any groups), which is important especially in kinematic analysis.

REFERENCES

Adler, C., Miyoshi-Akiyama, T., Aleman, L., Tanaka, M., Smith, J. and Mayer, B. (2000). Abl Family Kinases and Cbl Cooperate with the Nck Adaptor to Modulate Xenopus Development. *Journal of Biological Chemistry*, 275(46), pp.36472-36478.

Ahmed, G., Shinmyo, Y., Ohta, K., Islam, S., Hossain, M., Naser, I., Riyadh, A., Su, Y., Zhang, S., Tessier-Lavigne, M. and Tanaka, H. (2011). Draxin inhibits axonal outgrowth through the netrin receptor DCC. *Neuroscience Research*, 71, p.e67.

Al-Mosawie, A., Wilson, J. and Brownstone, R. (2007). Heterogeneity of V2-derived interneurons in the adult mouse spinal cord. *European Journal of Neuroscience*, 26(11), pp.3003-3015.

Alvarez, F., Jonas, P., Sapir, T., Hartley, R., Berrocal, M., Geiman, E., Todd, A. and Goulding, M. (2005). Postnatal phenotype and localization of spinal cord V1 derived interneurons. *The Journal of Comparative Neurology*, 493(2), pp.177-192.

Angel MJ, Guertin P, Jiminez I &McCrea DA (1996). Group I extensor afferents evoke disynaptic EPSPs in cat hindlimb extensor motoneurones during fictive locomotion. J Physiol **494**,851–861.

Arakawa, H. (2004). Netrin-1 and its receptors in tumorigenesis. *Nature Reviews Cancer*, 4(12), pp.978-987.

Arold, S., O'Brien, R., Franken, P., Strub, M., Hoh, F., Dumas, C. and Ladbury, J. (1998). RT Loop Flexibility Enhances the Specificity of Src Family SH3 Domains for HIV-1 Nef † , ‡. *Biochemistry*, 37(42), pp.14683-14691.

Bashaw, G. and Klein, R. (2010). Signaling from Axon Guidance Receptors. *Cold Spring Harbor Perspectives in Biology*, 2(5), pp.a001941-a001941.

Bellardita, C. and Kiehn, O. (2015). Phenotypic Characterization of Speed-Associated Gait Changes in Mice Reveals Modular Organization of Locomotor Networks. *Current Biology*, 25(11), pp.1426-1436.

Betley, J., Wright, C., Kawaguchi, Y., Erdélyi, F., Szabó, G., Jessell, T. and Kaltschmidt, J. (2009). Stringent Specificity in the Construction of a GABAergic Presynaptic Inhibitory Circuit. *Cell*, 139(1), pp.161-174.

Bisson, N., Poitras, L., Mikryukov, A., Tremblay, M. and Moss, T. (2007). EphA4 Signaling Regulates Blastomere Adhesion in the Xenopus Embryo by Recruiting

Pak1 to Suppress Cdc42 Function. *Molecular Biology of the Cell*, 18(3), pp.1030-1043.

Bladt, F., Aippersbach, E., Gelkop, S., Strasser, G., Nash, P., Tafuri, A., Gertler, F. and Pawson, T. (2003). The Murine Nck SH2/SH3 Adaptors Are Important for the Development of Mesoderm-Derived Embryonic Structures and for Regulating the Cellular Actin Network. *Molecular and Cellular Biology*, 23(13), pp.4586-4597.

Bong, Y., Park, Y., Lee, H., Mood, K., Ishimura, A. and Daar, I. (2004). Tyr-298 in ephrinB1 is critical for an interaction with the Grb4 adaptor protein. *Biochem. J.*, 377(2), pp.499-507.

Bredesen, D., Mehlen, P. and EI-Deiry, W. (2005). Receptors that mediate cellular dependence. *Cell Death Differ*, 12(8), pp.1031-1043.

Briancon-Marjollet, A., Ghogha, A., Nawabi, H., Triki, I., Auziol, C., Fromont, S., Piche, C., Enslen, H., Chebli, K., Cloutier, J., Castellani, V., Debant, A. and Lamarche-Vane, N. (2008). Trio Mediates Netrin-1-Induced Rac1 Activation in Axon Outgrowth and Guidance. *Molecular and Cellular Biology*, 28(7), pp.2314-2323.

Butt, S., Lundfald, L. and Kiehn, O. (2005). EphA4 defines a class of excitatory locomotor-related interneurons. *Proceedings of the National Academy of Sciences*, 102(39), pp.14098-14103.

Castellani, V. (2013). Building Spinal and Brain Commissures: Axon Guidance at the Midline. *ISRN Cell Biology*, 2013, pp.1-21.

Castets, M., Broutier, L., Molin, Y., Brevet, M., Chazot, G., Gadot, N., Paquet, A., Mazelin, L., Jarrosson-Wuilleme, L., Scoazec, J., Bernet, A. and Mehlen, P. (2011). DCC constrains tumour progression via its dependence receptor activity. *Nature*, 482(7386), pp.534-537.

Chan, S., Zheng, H., Su, M., Wilk, R., Killeen, M., Hedgecock, E. and Culotti, J. (1996). UNC-40, a C. elegans Homolog of DCC (Deleted in Colorectal Cancer), Is Required in Motile Cells Responding to UNC-6 Netrin Cues. *Cell*, 87(2), pp.187-195.

Charité, J., de Graaff, W., Vogels, R., Meijlink, F. and Deschamps, J. (1995). Regulation of the Hoxb-8 Gene: Synergism between Multimerized cis-Acting Elements Increases Responsiveness to Positional Information. *Developmental Biology*, 171(2), pp.294-305.

Chen, M., She, H., Davis, E., Spicer, C., Kim, L., Ren, R., Le Beau, M. and Li, W. (1998). Identification of Nck Family Genes, Chromosomal Localization, Expression, and Signaling Specificity. *Journal of Biological Chemistry*, 273(39), pp.25171-25178.

Chiang, C., Litingtung, Y., Lee, E., Young, K., Corden, J., Westphal, H. and Beachy, P. (1996). Cyclopia and defective axial patterning in mice lacking Sonic hedgehog gene function. *Nature*, 383(6599), pp.407-413.

Coleman, H., Labrador, J., Chance, R. and Bashaw, G. (2010). The Adam family metalloprotease Kuzbanian regulates the cleavage of the roundabout receptor to control axon repulsion at the midline. *Development*, 137(14), pp.2417-2426.

Conway BA, Hultborn H & Kiehn O (1987). Proprioceptive input resets central locomotor rhythm in the spinal cord. Exp Brain Res**68**, 643–656.

Conway BA, Scott DT, Riddell JS &Hadian MR (1994). Effects of plantar nerve stimulation on the transmission of late flexion reflexes in the decerebrate spinal cat. J Physiol **479.P**, 145P–146P.

Cowan, C. and Henkemeyer, M. (2001). The Sh2/Sh3 Adaptor Grb4 Transduces B-Ephrin Reverse Signals. *Nature*, 413(6852), pp.174-179.

Crone, S., Quinlan, K., Zagoraiou, L., Droho, S., Restrepo, C., Lundfald, L., Endo, T., Setlak, J., Jessell, T., Kiehn, O. and Sharma, K. (2008). Genetic Ablation of V2a Ipsilateral Interneurons Disrupts Left-Right Locomotor Coordination in Mammalian Spinal Cord. *Neuron*, 60(1), pp.70-83.

Crone, S., Zhong, G., Harris-Warrick, R. and Sharma, K. (2009). In Mice Lacking V2a Interneurons, Gait Depends on Speed of Locomotion. *Journal of Neuroscience*, 29(21), pp.7098-7109.

Depienne, C., Cincotta, M., Billot, S., Bouteiller, D., Groppa, S., Brochard, V., Flamand, C., Hubsch, C., Meunier, S., Giovannelli, F., Klebe, S., Corvol, J., Vidailhet, M., Brice, A. and Roze, E. (2011). A novel DCC mutation and genetic heterogeneity in congenital mirror movements. *Neurology*, 76(3), pp.260-264.

Donelan JM & Pearson KG (2004).Contribution of force feedback to ankle extensor activity in decerebrate walking cats. J Neurophysiol **92**, 2093–2104.

Dougherty, K. and Kiehn, O. (2010). Firing and Cellular Properties of V2a Interneurons in the Rodent Spinal Cord. *Journal of Neuroscience*, 30(1), pp.24-37.

Dougherty, K. and Kiehn, O. (2010). Functional organization of V2a-related locomotor circuits in the rodent spinal cord. *Annals of the New York Academy of Sciences*, 1198(1), pp.85-93.

Drew T, Prentice S, Schepens B (2004) Cortical and brainstem control of locomotion. *Prog Brain Res* 143, pp.0079-6123.

Duysens J & Pearson KG (1980).Inhibition of flexor burst generation by loading ankle extensor muscles in walking cats.Brain Res **187**, 321–332.

Endo, T. and Kiehn, O. (2008). Asymmetric Operation of the Locomotor Central Pattern Generator in the Neonatal Mouse Spinal Cord. *Journal of Neurophysiology*, 100(6), pp.3043-3054.

Fan, X., Labrador, J., Hing, H. and Bashaw, G. (2003). Slit Stimulation Recruits Dock and Pak to the Roundabout Receptor and Increases Rac Activity to Regulate Axon Repulsion at the CNS Midline. *Neuron*, 40(1), pp.113-127.

Fawcett, J., Georgiou, J., Ruston, J., Bladt, F., Sherman, A., Warner, N., Saab, B., Scott, R., Roder, J. and Pawson, T. (2007). Nck adaptor proteins control the organization of neuronal circuits important for walking. *Proceedings of the National Academy of Sciences*, 104(52), pp.20973-20978.

Fazeli, A., Dickinson, S., Hermiston, M., Tighe, R., Steen, R., Small, C., Stoeckli, E., Keino-Masu, K., Masu, M., Rayburn, H., Simons, J., Bronson, R., Gordon, J., Tessier-Lavigne, M. and Weinberg, R. (1997). Phenotype of mice lacking functional Deleted in colorectal cancer (Dec) gene. *Nature*, 386(6627), pp.796-804.

Finci, L., Krüger, N., Sun, X., Zhang, J., Chegkazi, M., Wu, Y., Schenk, G., Mertens, H., Svergun, D., Zhang, Y., Wang, J. and Meijers, R. (2014). The Crystal Structure of Netrin-1 in Complex with DCC Reveals the Bifunctionality of Netrin-1 As a Guidance Cue. *Neuron*, 83(4), pp.839-849.

Finci, L., Zhang, Y., Meijers, R. and Wang, J. (2015). Signaling mechanism of the netrin-1 receptor DCC in axon guidance. *Progress in Biophysics and Molecular Biology*, 118(3), pp.153-160.

Fothergill, T., Donahoo, A., Douglass, A., Zalucki, O., Yuan, J., Shu, T., Goodhill, G. and Richards, L. (2013). Netrin-DCC Signaling Regulates Corpus Callosum Formation Through Attraction of Pioneering Axons and by Modulating Slit2-Mediated Repulsion. *Cerebral Cortex*, 24(5), pp.1138-1151.

Franz, E., Chiaroni-Clarke, R., Woodrow, S., Glendining, K., Jasoni, C., Robertson, S., Gardner, R. and Markie, D. (2015). Congenital mirror movements: Phenotypes associated with DCC and RAD51 mutations. *Journal of the Neurological Sciences*, 351(1-2), pp.140-145.

Frese, S., Schubert, W., Findeis, A., Marquardt, T., Roske, Y., Stradal, T. and Heinz, D. (2006). The Phosphotyrosine Peptide Binding Specificity of Nck1 and Nck2 Src Homology 2 Domains. *Journal of Biological Chemistry*, 281(26), pp.18236-18245.

Gad, J., Keeling, S., Wilks, A., Tan, S. and Cooper, H. (1997). The Expression Patterns of Guidance Receptors, DCC and Neogenin, Are Spatially and Temporally Distinct throughout Mouse Embryogenesis. *Developmental Biology*, 192(2), pp.258-273.

Goldschneider, D. and Mehlen, P. (2010). Dependence receptors: a new paradigm in cell signaling and cancer therapy. *Oncogene*, 29(13), pp.1865-1882.

Gosgnach, S., Lanuza, G., Butt, S., Saueressig, H., Zhang, Y., Velasquez, T., Riethmacher, D., Callaway, E., Kiehn, O. and Goulding, M. (2006). V1 spinal neurons regulate the speed of vertebrate locomotor outputs. *Nature*, 440(7081), pp.215-219.

Gossard J-P, Brownstone RM,Barajon I & Hultborn H (1994).Transmission in a locomotor-related group Ib pathway from hindlimb extensor muscles in the cat. Exp Brain Res **98**, 213–228.

Goulding, M. (2009). Circuits controlling vertebrate locomotion: moving in a new direction. *Nature Reviews Neuroscience*, 10(7), pp.507-518.

Grillner S (1981). Control of locomotion in bipeds, tetrapods, and fish. In *Handbook of Physiology. The Nervous System.*, vol. **II**, p. 2, chap. 26 *Motor Control*, ed. Brookhart JM &Mountcastle VB, pp. 1179–1236. American Physiological Society, Bethesda .

Grillner, S. (2003). The motor infrastructure: from ion channels to neuronal networks. *Nature Reviews Neuroscience*, 4(7), pp.573-586.

Gross, M., Dottori, M. and Goulding, M. (2002). Lbx1 Specifies Somatosensory Association Interneurons in the Dorsal Spinal Cord. *Neuron*, 34(4), pp.535-549.

Guertin P, Angel MJ, Perreault M-C & McCrea DA (1995). Ankle extensor group I afferents excite extensors throughout the hindlimb during fictive locomotion in the cat. J Physiol**487**, 197–209.

Haddick, P., Tom, I., Luis, E., Quiñones, G., Wranik, B., Ramani, S., Stephan, J., Tessier-Lavigne, M. and Gonzalez, L. (2014). Defining the Ligand Specificity of the Deleted in Colorectal Cancer (DCC) Receptor. *PLoS ONE*, 9(1), p.e84823.

Hiebert GW, Whelan PJ,Prochazka A & Pearson KG (1996).Contribution of hind limb flexor muscle afferents to the timing of phase transitions in the cat step cycle. J Neurophysiol **75**,1126–1137.

Hock, B., Bohme, B., Karn, T., Yamamoto, T., Kaibuchi, K., Holtrich, U., Holland, S., Pawson, T., Rubsamen-Waigmann, H. and Strebhardt, K. (1998). PDZ-domain-mediated interaction of the Eph-related receptor tyrosine kinase EphB3 and the ras-binding protein AF6 depends on the kinase activity of the receptor. *Proceedings of the National Academy of Sciences*, 95(17), pp.9779-9784.

Holland, S., Gale, N., Gish, G., Roth, R., Songyang, Z., Cantley, L., Henkemeyer, M., Yancopoulos, G. and Pawson, T. (1997). Juxtamembrane tyrosine residues couple the Eph family receptor EphB2/Nuk to specific SH2 domain proteins in neuronal cells. *EMBO J*, 16(13), pp.3877-3888.

Hong, K., Hinck, L., Nishiyama, M., Poo, M., Tessier-Lavigne, M. and Stein, E. (1999). A Ligand-Gated Association between Cytoplasmic Domains of UNC5 and DCC Family Receptors Converts Netrin-Induced Growth Cone Attraction to Repulsion. *Cell*, 97(7), pp.927-941.

Horn, K., Glasgow, S., Gobert, D., Bull, S., Luk, T., Girgis, J., Tremblay, M., McEachern, D., Bouchard, J., Haber, M., Hamel, E., Krimpenfort, P., Murai, K., Berns, A., Doucet, G., Chapman, C., Ruthazer, E. and Kennedy, T. (2013). DCC Expression by Neurons Regulates Synaptic Plasticity in the Adult Brain. *Cell Reports*, 3(1), pp.173-185.

Islam, S., Shinmyo, Y., Okafuji, T., Su, Y., Naser, I., Ahmed, G., Zhang, S., Chen, S., Ohta, K., Kiyonari, H., Abe, T., Tanaka, S., Nishinakamura, R., Terashima, T., Kitamura, T. and Tanaka, H. (2009). Draxin, a Repulsive Guidance Protein for Spinal Cord and Forebrain Commissures. *Science*, 323(5912), pp.388-393.

Jankowska E, Jukes MGM, Lund S& Lundberg A (1967). The effect of DOPA on the spinal cord. VI. Half-centre organization of interneurones transmitting effects from the flexor reflex afferents. Acta Physiol Scand **70**,389–402.

Jessell, T. (2000). Neuronal specification in the spinal cord: inductive signals and transcriptional codes. *Nat Rev Genet*, 1(1), pp.20-29.

Jones, N., Blasutig, I., Eremina, V., Ruston, J., Bladt, F., Li, H., Huang, H., Larose, L., Li, S., Takano, T., Quaggin, S. and Pawson, T. (2006). Nck adaptor proteins link nephrin to the actin cytoskeleton of kidney podocytes. *Nature*, 440(7085), pp.818-823.

Jordan, L. (1998). Initiation of Locomotion in Mammals. *Annals of the New York Academy of Sciences*, 860(1 NEURONAL MECH), pp.83-93.

Kadison, S. (2006). EphB Receptors and Ephrin-B3 Regulate Axon Guidance at the Ventral Midline of the Embryonic Mouse Spinal Cord. *Journal of Neuroscience*, 26(35), pp.8909-8914.

Kaneko, T., Huang, H., Zhao, B., Li, L., Liu, H., Voss, C., Wu, C., Schiller, M. and Li, S. (2010). Loops Govern SH2 Domain Specificity by Controlling Access to Binding Pockets. *Science Signaling*, 3(120), pp.ra34-ra34.

Karunaratne, A., Hargrave, M., Poh, A. and Yamada, T. (2002). GATA Proteins Identify a Novel Ventral Interneuron Subclass in the Developing Chick Spinal Cord. *Developmental Biology*, 249(1), pp.30-43.

Keino-Masu, K., Masu, M., Hinck, L., Leonardo, E., Chan, S., Culotti, J. and Tessier-Lavigne, M. (1996). Deleted in Colorectal Cancer (DCC) Encodes a Netrin Receptor. *Cell*, 87(2), pp.175-185.

Kennedy, T. (2006). Axon Guidance by Diffusible Chemoattractants: A Gradient of Netrin Protein in the Developing Spinal Cord. *Journal of Neuroscience*, 26(34), pp.8866-8874.

Kennedy, T., Serafini, T., de la Torre, J. and Tessier-Lavigne, M. (1994). Netrins are diffusible chemotropic factors for commissural axons in the embryonic spinal cord. *Cell*, 78(3), pp.425-435.

Kiehn, O., Dougherty, K., Hägglund, M., Borgius, L., Talpalar, A. and Restrepo, C. (2010). Probing spinal circuits controlling walking in mammals. *Biochemical and Biophysical Research Communications*, 396(1), pp.11-18.

Kimura, Y. (2006). alx, a Zebrafish Homolog of Chx10, Marks Ipsilateral Descending Excitatory Interneurons That Participate in the Regulation of Spinal Locomotor Circuits. *Journal of Neuroscience*, 26(21), pp.5684-5697.

Kolodziej, P., Timpe, L., Mitchell, K., Fried, S., Goodman, C., Jan, L. and Jan, Y. (1996). frazzled Encodes a Drosophila Member of the DCC Immunoglobulin Subfamily and Is Required for CNS and Motor Axon Guidance. *Cell*, 87(2), pp.197-204.

Krimpenfort, P., Song, J., Proost, N., Zevenhoven, J., Jonkers, J. and Berns, A. (2012). Deleted in colorectal carcinoma suppresses metastasis in p53-deficient mammary tumours. *Nature*, 482(7386), pp.538-541.

Kullander, K. (2003). Role of EphA4 and EphrinB3 in Local Neuronal Circuits That Control Walking. *Science*, 299(5614), pp.1889-1892.

Kullander, K., Mather, N., Diella, F., Dottori, M., Boyd, A. and Klein, R. (2001). Kinase-Dependent and Kinase-Independent Functions of EphA4 Receptors in Major Axon Tract Formation In Vivo. *Neuron*, 29(1), pp.73-84.

Lane, C., Qi, J. and Fawcett, J. (2015). NCK is critical for the development of deleted in colorectal cancer (DCC) sensitive spinal circuits. *J. Neurochem.*, 134(6), pp.1008-1014.

Lanuza, G., Gosgnach, S., Pierani, A., Jessell, T. and Goulding, M. (2004). Genetic Identification of Spinal Interneurons that Coordinate Left-Right Locomotor Activity Necessary for Walking Movements. *Neuron*, 42(3), pp.375-386.

Lawrence, D. and Kuypers, H. (1968a). The Functional Organization of the Motor System in the Monkey. *Brain*, 91(1), pp.1-14.

Lawrence, D. and Kuypers, H. (1968b). The Functional Organization of the Motor System in the Monkey. *Brain*, 91(1), pp.15-36.

Leblond H, L'Esperance M, Orsal D, Rossignol S (2003). Theadmill locomotion in the intact and spinal mouse. *J Neurosci.* 23(36), pp.11411-11419.

Lee, R., Petros, T. and Mason, C. (2008). Zic2 Regulates Retinal Ganglion Cell Axon Avoidance of ephrinB2 through Inducing Expression of the Guidance Receptor EphB1. *Journal of Neuroscience*, 28(23), pp.5910-5919.

Lehmann, J., Riethmüller, G. and Johnson, J. (1990). Nck, a melanoma cDNA encoding a cytoplasmic protein consisting of the src homology units SH2 and SH3. *Nucl Acids Res*, 18(4), pp.1048-1048.

Leonardo, E., Hinck, L., Masu, M., Keino-Masu, K., Ackerman, S. and Tessier-Lavigne, M. (1997). Vertebrate homologues of C. elegans UNC-5 are candidate netrin receptors. *Nature*, 386(6627), pp.833-838.

Leung-Hagesteijn, C., Spence, A., Stern, B., Zhou, Y., Su, M., Hedgecock, E. and Culotti, J. (1992). UNC-5, a transmembrane protein with immunoglobulin and

thrombospondin type 1 domains, guides cell and pioneer axon migrations in C. elegans. *Cell*, 71(2), pp.289-299.

Li, W., Fan, J. and Woodley, D. (2001). Nck/Dock: an adapter between cell surface receptors and the actin cytoskeleton. *Oncogene*, 20(44), pp.6403-6417.

Li, W., Lee, J., Vikis, H., Lee, S., Liu, G., Aurandt, J., Shen, T., Fearon, E., Guan, J., Han, M., Rao, Y., Hong, K. and Guan, K. (2004). Activation of FAK and Src are receptor-proximal events required for netrin signaling. *Nature Neuroscience*, 7(11), pp.1213-1221.

Li, X. (2002). The Adaptor Protein Nck-1 Couples the Netrin-1 Receptor DCC (Deleted in Colorectal Cancer) to the Activation of the Small GTPase Rac1 through an Atypical Mechanism. *Journal of Biological Chemistry*, 277(40), pp.37788-37797.

Liem, K., Tremml, G. and Jessell, T. (1997). A Role for the Roof Plate and Its Resident TGFβ-Related Proteins in Neuronal Patterning in the Dorsal Spinal Cord. *Cell*, 91(1), pp.127-138.

Long, H., Sabatier, C., Le Ma, Plump, A., Yuan, W., Ornitz, D., Tamada, A., Murakami, F., Goodman, C. and Tessier-Lavigne, M. (2004). Conserved Roles for Slit and Robo Proteins in Midline Commissural Axon Guidance. *Neuron*, 42(2), pp.213-223.

Lundfald, L., Restrepo, C., Butt, S., Peng, C., Droho, S., Endo, T., Zeilhofer, H., Sharma, K. and Kiehn, O. (2007). Phenotype of V2-derived interneurons and their relationship to the axon guidance molecule EphA4 in the developing mouse spinal cord. *European Journal of Neuroscience*, 26(11), pp.2989-3002.

McCrea DA (2001). Spinal circuitry of sensorimotor control of locomotion. J Physiol **533**, 41–50.

Mehlen, P. and Furne, C. (2005). Netrin-1: when a neuronal guidance cue turns out to be a regulator of tumorigenesis. *Cell. Mol. Life Sci.*, 62(22), pp.2599-2616.

Meneret, A., Depienne, C., Riant, F., Trouillard, O., Bouteiller, D., Cincotta, M., Bitoun, P., Wickert, J., Lagroua, I., Westenberger, A., Borgheresi, A., Doummar, D., Romano, M., Rossi, S., Defebvre, L., De Meirleir, L., Espay, A., Fiori, S., Klebe, S., Quelin, C., Rudnik-Schoneborn, S., Plessis, G., Dale, R., Sklower Brooks, S., Dziezyc, K., Pollak, P., Golmard, J., Vidailhet, M., Brice, A. and Roze, E. (2014). Congenital mirror movements: Mutational analysis of RAD51 and DCC in 26 cases. *Neurology*, 82(22), pp.1999-2002.

Meyerhardt, J., Look, A., Bigner, S. and Fearon, E. (1997). Identification and characterization of neogenin, a DCC-related gene. *Oncogene*, 14(10), pp.1129-1136.

Mohamed, A., Boudreau, J., Yu, F., Liu, J. and Chin-Sang, I. (2012). The Caenorhabditis elegans Eph Receptor Activates NCK and N-WASP, and Inhibits Ena/VASP to Regulate Growth Cone Dynamics during Axon Guidance. *PLoS Genetics*, 8(2), p.e1002513.

Moran-Rivard, L., Kagawa, T., Saueressig, H., Gross, M., Burrill, J. and Goulding, M. (2001). Evx1 Is a Postmitotic Determinant of V0 Interneuron Identity in the Spinal Cord. *Neuron*, 29(2), pp.385-399.

Müller, T., Brohmann, H., Pierani, A., Heppenstall, P., Lewin, G., Jessell, T. and Birchmeier, C. (2002). The Homeodomain Factor Lbx1 Distinguishes Two Major Programs of Neuronal Differentiation in the Dorsal Spinal Cord. *Neuron*, 34(4), pp.551-562.

Nishimaru, H. and Kakizaki, M. (2009). The role of inhibitory neurotransmission in locomotor circuits of the developing mammalian spinal cord. *Acta Physiologica*, 197(2), pp.83-97.

Oosterveen, T. (2003). Retinoids regulate the anterior expression boundaries of 5' Hoxb genes in posterior hindbrain. *The EMBO Journal*, 22(2), pp.262-269.

Orlovsky GN, Deliagina T &Grillner S (1999). *Neuronal Control of Locomotion: from Mollusc to Man*. Oxford University Press, New York .

Pawson, T., Gish, G. and Nash, P. (2001). SH2 domains, interaction modules and cellular wiring. *Trends in Cell Biology*, 11(12), pp.504-511.

Pearson KG & Collins DF (1993).Reversal of the influence of group Ib afferents from plantaris on activity in medial gastrocnemius muscle during locomotor activity.J Neurophysiol **70**, 1009–1017.

Pearson KG (2004). Generating the walking gait: role of sensory feedback. Prog Brain Res **143**, pp.123–129.

Pearson, K., Acharya, H. and Fouad, K. (2005). A new electrode configuration for recording electromyographic activity in behaving mice. *Journal of Neuroscience Methods*, 148(1), pp.36-42.

Peng, C., Yajima, H., Burns, C., Zon, L., Sisodia, S., Pfaff, S. and Sharma, K. (2007). Notch and MAML Signaling Drives Scl-Dependent Interneuron Diversity in the Spinal Cord. *Neuron*, 53(6), pp.813-827.

Perreault M, Angel MJ, Guertin P& McCrea DA (1995). Effects of stimulation of hindlimb flexor group II afferents during fictive locomotion in the cat. J Physiol**487**, 211–220.

Philipp, M., Niederkofler, V., Debrunner, M., Alther, T., Kunz, B. and Stoeckli, E. (2012). RabGDI controls axonal midline crossing by regulating Robo1 surface expression. *Neural Dev*, 7(1), p.36.

Phillipson M (1905) L'autonomie et la centralization dans le systeme nerveux des animaux. *Travails du Laboratoire de la Physiologie, Institut Solvey*. 7, pp.1–208.

Pierani, A., Moran-Rivard, L., Sunshine, M., Littman, D., Goulding, M. and Jessell, T. (2001). Control of Interneuron Fate in the Developing Spinal Cord by the Progenitor Homeodomain Protein Dbx1. *Neuron*, 29(2), pp.367-384.

Pramatarova, A., Ochalski, P., Chen, K., Gropman, A., Myers, S., Min, K. and Howell, B. (2003). Nck Interacts with Tyrosine-Phosphorylated Disabled 1 and Redistributes in Reelin-Stimulated Neurons. *Molecular and Cellular Biology*, 23(20), pp.7210-7221.

Quevedo J, Fedirchuk B,Gosgnach S & McCrea DA (2000).Group I disynaptic excitation of cat hindlimb flexor and bifunctional motoneurones during fictive locomotion. J Physiol**525**, 549–564.

Quevedo J, Stecina K, Gosgnach S& McCrea DA (2005a). Stumbling corrective reaction during fictive locomotion in the cat. J Neurophysiol **94**, 2045–2052.

Rabe Bernhardt, N., Memic, F., Gezelius, H., Thiebes, A., Vallstedt, A. and Kullander, K. (2012). DCC mediated axon guidance of spinal interneurons is essential for normal locomotor central pattern generator function. *Developmental Biology*, 366(2), pp.279-289.

Rabe, N., Gezelius, H., Vallstedt, A., Memic, F. and Kullander, K. (2009). Netrin-1-Dependent Spinal Interneuron Subtypes Are Required for the Formation of Left-Right Alternating Locomotor Circuitry. *Journal of Neuroscience*, 29(50), pp.15642-15649.

Raper, J. and Mason, C. (2010). Cellular Strategies of Axonal Pathfinding. *Cold Spring Harbor Perspectives in Biology*, 2(9), pp.a001933-a001933.

Ren, R., Mayer, B., Cicchetti, P. and Baltimore, D. (1993). Identification of a ten-amino acid proline-rich SH3 binding site. *Science*, 259(5098), pp.1157-1161.

Ren, X., Ming, G., Xie, Y., Hong, Y., Sun, D., Zhao, Z., Feng, Z., Wang, Q., Shim, S., Chen, Z., Song, H., Mei, L. and Xiong, W. (2004). Focal adhesion kinase in netrin-1 signaling. *Nature Neuroscience*, 7(11), pp.1204-1212.

Rossignol S (1996). Neural control of stereotypic limb movements. In *Handbook of Physiology*, chap. 12, ed. Rowell LB & Shepherd J, pp. 173–216. American Physiological Society, Bethesda .

Rossignol S, Dubuc R & Gossard J-P (2006). Dynamic sensorimotor interactions in locomotion. Physiol Rev **86**, 89–154.

Rossignol S, Dubuc R & Gossard J-P (2006). Dynamic sensorimotor interactions in locomotion. Physiol Rev **86**, 89–154.

Rossignol, S. (1996). Visuomotor regulation of locomotion. *Canadian Journal of Physiology and Pharmacology*, 74(4), pp.418-425.

Round, J. and Sun, H. (2011). The adaptor protein Nck2 mediates Slit1-induced changes in cortical neuron morphology. *Molecular and Cellular Neuroscience*, 47(4), pp.265-273.

Sapir, T. (2004). Pax6 and Engrailed 1 Regulate Two Distinct Aspects of Renshaw Cell Development. *Journal of Neuroscience*, 24(5), pp.1255-1264.

Saueressig, H., Burrill, J. and Goulding, M. (1999). Engrailed-1 and netrin-1 regulate axon pathfinding by association interneurons that project to motor neurons. *Development*, 126(19), pp.4201-4212.

Saxena, K., Tamm, L., Walley, A., Simmons, A., Rollins, N., Chia, J., Soares, J., Emslie, G., Fan, X. and Huang, H. (2012). A Preliminary Investigation of Corpus Callosum and Anterior Commissure Aberrations in Aggressive Youth with Bipolar Disorders. *Journal of Child and Adolescent Psychopharmacology*, 22(2), pp.112-119.

Serafini, T., Colamarino, S., Leonardo, E., Wang, H., Beddington, R., Skarnes, W. and Tessier-Lavigne, M. (1996). Netrin-1 Is Required for Commissural Axon Guidance in the Developing Vertebrate Nervous System. *Cell*, 87(6), pp.1001-1014.

Serafini, T., Kennedy, T., Gaiko, M., Mirzayan, C., Jessell, T. and Tessier-Lavigne, M. (1994). The netrins define a family of axon outgrowth-promoting proteins homologous to C. elegans UNC-6. *Cell*, 78(3), pp.409-424.

Shekarabi, M. (2005). Deleted in Colorectal Cancer Binding Netrin-1 Mediates Cell Substrate Adhesion and Recruits Cdc42, Rac1, Pak1, and N-WASP into an Intracellular Signaling Complex That Promotes Growth Cone Expansion. *Journal of Neuroscience*, 25(12), pp.3132-3141.

Siembab, V., Smith, C., Zagoraiou, L., Berrocal, M., Mentis, G. and Alvarez, F. (2010). Target selection of proprioceptive and motor axon synapses on neonatal V1-derived Ia inhibitory interneurons and Renshaw cells. *The Journal of Comparative Neurology*, 518(23), pp.4675-4701.

Srour, M., Philibert, M., Dion, M., Duquette, A., Richer, F., Rouleau, G. and Chouinard, S. (2009). Familial Congenital Mirror Movements: Report of a Large 4-Generration Family. *Neurology*, 73(9), pp.729-731.

Srour, M., Riviere, J., Pham, J., Dube, M., Girard, S., Morin, S., Dion, P., Asselin, G., Rochefort, D., Hince, P., Diab, S., Sharafaddinzadeh, N., Chouinard, S., Theoret, H., Charron, F. and Rouleau, G. (2010). Mutations in DCC Cause Congenital Mirror Movements. *Science*, 328(5978), pp.592-592.

Stecina K, Quevedo J & McCrea DA (2005). Parallel reflex pathways from flexor muscle afferents evoking resetting and flexion enhancement during fictive locomotion and scratch in the cat. J Physiol **569**, 275–290.

Stein, E. (2001). Binding of DCC by Netrin-1 to Mediate Axon Guidance Independent of Adenosine A2B Receptor Activation. *Science*, 291(5510), pp.1976-1982.

Stein, E., Huynh-Do, U., Lane, A., Cerretti, D. and Daniel, T. (1998). Nck Recruitment to Eph Receptor, EphB1/ELK, Couples Ligand Activation to c-Jun Kinase. *Journal of Biological Chemistry*, 273(3), pp.1303-1308.

Talpalar, A., Bouvier, J., Borgius, L., Fortin, G., Pierani, A. and Kiehn, O. (2013). Dual-mode operation of neuronal networks involved in left–right alternation. *Nature*, 500(7460), pp.85-88.

Timmer, J., Wang, C. and Niswander, L. (2002). BMP signaling patterns the dorsal and intermediate neural tube via regulation of homeobox and helix-loop-helix transcription factors. *Development*, 129(10), pp.2459–2472.

Valarche, I., de Graaff, W. and Deschamps, J. (1997). A 3' remote control region is a candidate to modulate Hoxb-8 expression boundaries. *International Journal of Developmental Biology*, 41(5), pp.705–714.

Vitriol, E. and Zheng, J. (2012). Growth Cone Travel in Space and Time: the Cellular Ensemble of Cytoskeleton, Adhesion, and Membrane. *Neuron*, 73(6), pp.1068-1081.

Wang, Z., Li, L., Goulding, M. and Frank, E. (2008). Early Postnatal Development of Reciprocal Ia Inhibition in the Murine Spinal Cord. *Journal of Neurophysiology*, 100(1), pp.185-196.

Whelan, P. (1996). Control of Locomotion in the Decerebrate Cat. *Progress in Neurobiology*, 49(5), pp.481-515.

Wilson, J., Blagovechtchenski, E. and Brownstone, R. (2010). Genetically Defined Inhibitory Neurons in the Mouse Spinal Cord Dorsal Horn: A Possible Source of Rhythmic Inhibition of Motoneurons during Fictive Locomotion. *Journal of Neuroscience*, 30(3), pp.1137-1148.

Witschi, R., Johansson, T., Morscher, G., Scheurer, L., Deschamps, J. and Zeilhofer, H. (2010). Hoxb8-Cre mice: A tool for brain-sparing conditional gene deletion. *genesis*, 48(10), pp.596-602.

Wunderlich, L. (1999). Requirement of multiple SH3 domains of Nck for ligand binding. *Cellular Signalling*, 11(4), pp.253-262.

Xu, N. and Henkemeyer, M. (2009). Ephrin-B3 reverse signaling through Grb4 and cytoskeletal regulators mediates axon pruning. *Nature Neuroscience*, 12(3), pp.268-276.

Xu, N., Sun, S., Gibson, J. and Henkemeyer, M. (2011). A dual shaping mechanism for postsynaptic ephrin-B3 as a receptor that sculpts dendrites and synapses. *Nature Neuroscience*, 14(11), pp.1421-1429.

Yang, L. and Bashaw, G. (2006). Son of Sevenless Directly Links the Robo Receptor to Rac Activation to Control Axon Repulsion at the Midline. *Neuron*, 52(4), pp.595-607.

Yokoyama, N., Romero, M., Cowan, C., Galvan, P., Helmbacher, F., Charnay, P., Parada, L. and Henkemeyer, M. (2001). Forward Signaling Mediated by Ephrin-B3 Prevents Contralateral Corticospinal Axons from Recrossing the Spinal Cord Midline. *Neuron*, 29(1), pp.85-97.

Yu, T., Hao, J., Lim, W., Tessier-Lavigne, M. and Bargmann, C. (2002). Shared receptors in axon guidance: SAX-3/Robo signals via UNC-34/Enabled and a Netrin-independent UNC-40/DCC function. *Nature Neuroscience*, 5(11), pp.1147-1154.

Yuasa-Kawada, J., Kinoshita-Kawada, M., Wu, G., Rao, Y. and Wu, J. (2009). Midline crossing and Slit responsiveness of commissural axons require USP33. *Nature Neuroscience*, 12(9), pp.1087-1089.

Zehr EP & Duysens J (2004).Regulation of arm and leg movement during human locomotion. Neuroscientist **4**,347–361.

Zhang, J., Lanuza, G., Britz, O., Wang, Z., Siembab, V., Zhang, Y., Velasquez, T., Alvarez, F., Frank, E. and Goulding, M. (2014). V1 and V2b Interneurons Secure the Alternating Flexor-Extensor Motor Activity Mice Require for Limbed Locomotion. *Neuron*, 82(1), pp.138-150.

Zhang, Y., Narayan, S., Geiman, E., Lanuza, G., Velasquez, T., Shanks, B., Akay, T., Dyck, J., Pearson, K., Gosgnach, S., Fan, C. and Goulding, M. (2008). V3 Spinal Neurons Establish a Robust and Balanced Locomotor Rhythm during Walking. *Neuron*, 60(1), pp.84-96.

Zhong, G., Droho, S., Crone, S., Dietz, S., Kwan, A., Webb, W., Sharma, K. and Harris-Warrick, R. (2010). Electrophysiological Characterization of V2a Interneurons and Their Locomotor-Related Activity in the Neonatal Mouse Spinal Cord. *Journal of Neuroscience*, 30(1), pp.170-182.